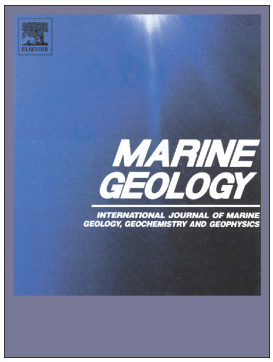

Controls on the formation of turbidity current channels associated with marine-terminating glaciers and ice sheets

Ed L. Pope, Alexandre Normandeau, Colm Ó. Cofaigh, Chris R. Stokes, Peter J. Talling

PII: S0025-3227(19)30071-4
DOI: https://doi.org/10.1016/j.margeo.2019.05.010
Reference: MARGO 5951

To appear in: *Marine Geology*

Received date: 11 February 2019
Revised date: 22 May 2019
Accepted date: 26 May 2019

Please cite this article as: E.L. Pope, A. Normandeau, C.Ó. Cofaigh, et al., Controls on the formation of turbidity current channels associated with marine-terminating glaciers and ice sheets, Marine Geology, https://doi.org/10.1016/j.margeo.2019.05.010

Controls on the formation of turbidity current channels associated with marine-terminating glaciers and ice sheets

Ed L. Pope[1*], Alexandre Normandeau[2], Colm Ó Cofaigh[1], Chris R. Stokes[1], Peter J. Talling[3]

[1]Department of Geography, Durham University, Science Laboratories, South Road, Durham, DH1 3LE, UK

[2]Geological Survey of Canada (Atlantic), Bedford Institute of Oceanography, Dartmouth, NS, B2Y 4A2, Canada

[3]Departments of Earth Science and Geography, Durham University, Science Laboratories, South Road, Durham, DH1 3LE, UK

Keywords: submarine channels, fjords, ice sheets, turbidity currents, geomorphology, glacimarine processes

Abstract

Submarine channels, and the sediment density flows which form them, act as conduits for the transport of sediment, macro-nutrients, fresher water and organic matter from the coast to the deep sea. These systems are therefore significant pathways for global sediment and carbon cycles. However, the conditions that permit or preclude submarine channel formation are poorly understood, especially when in association with marine-terminating glaciers. Here, using swath-bathymetric data from the inner shelf and fjords of northwest and southeast Greenland, we provide the first paper to analyse the controls on the formation of submarine channels offshore of numerous marine-terminating glaciers. These data reveal 37 submarine channels: 11 offshore of northwest Greenland and 26 offshore of southeast Greenland. The presence of channels is nearly always associated with: (1) a stable glacier front, as indicated by the association with either a moraine or grounding-zone wedge; and (2), a consistent seaward sloping gradient. In northwest Greenland, turbidity current channels are also more likely to be associated with larger glacier catchments with higher ice and meltwater fluxes which provide higher volumes of sediment delivery. However, the factors controlling the presence of channels in northwest and southeast Greenland are different, which suggest some complexity about predicting the occurrence of turbidity currents in glacier-influenced settings. Future work on tidewater glacier sediment delivery rates by different subglacial processes, and the role of grain size and catchment/regional geology is required to address uncertainties regarding the controls on channel formation.

*Corresponding Author: edward.pope@durham.ac.uk

1. Introduction

Submarine channels are a common feature of the world's oceans where large volumes of sediment are introduced into coastal waters, or where continental shelf and slope processes are episodic, such as related to the advance and retreat of ice sheets (Peakall et al., 2000; Ó Cofaigh et al., 2004; 2006; Wynn et al., 2007; Lastras et al., 2009; Conway et al., 2012). These channels, and the sediment density flows which form them, act as conduits for the transport of sediment, macro-nutrients, fresher water and organic matter from coastal environments to deeper water (Canals et al., 2006; Galy et al., 2007; Kao et al., 2010; Azpiroz-Zabala et al., 2017; Amblas et al., 2018).

Here, we present an initial study of why submarine channels are found in some locations, but not in others, determining the controls on their presence or absence. Similar questions have long been asked for river systems on land, where channel presence is determined by surface gradients and the amount and pattern of accumulation of surface rainfall and runoff (Leopold and Wolman, 1957; Schumm and Lichty, 1965; Lane and Richards, 1997). Similar processes do not occur underwater, and submarine channels also terminate, unlike river channels that typically extend continuously to the shorelines. There are few previous studies that have quantitatively analysed seafloor bathymetry to determine controls on submarine channel occurrence, but the recent availability of swath bathymetry data over large areas now makes such work possible (Kneller, 2003; Mitchell, 2005; Amblas et al., 2015). Past analysis of submarine channels has been restricted to their geometry and internal processes (Clark et al., 1992; Clark and Pickering, 1996; Peakall et al., 2000; Konsoer et al., 2013; Peakall and Sumner, 2015), rather than why they exist. In this contribution, we consider submarine channels offshore from glaciated margins.

Submarine channels are commonly found offshore the world's largest rivers (Clark and Pickering, 1996). Here, the presence of a channel is commonly linked to rapid deposition of large volumes of sediment on sufficiently steep offshore gradients, leading to slope failure or the plunging of river flood

water. However, the exact conditions that permit or prevent submarine channel formation in these locations remains poorly understood. In contrast to the world's largest rivers, large submarine channels are less commonly associated with the offshore sediment depocentres of the world's largest ice streams (Dowdeswell et al., 1996; Pope et al., 2018). Despite the rapid delivery of exceptionally large volumes of sediment, these trough-mouth fans are thought to be constructed through recurrent glacigenic debris-flow occurrence (Vorren and Laberg, 1997). Where channels are found, they are often hypothesised to be a consequence of meltwater sedimentation (Ó Cofaigh et al., 2018; Pope et al., 2018; Rui et al., 2019). Despite their rarity, however, perhaps the world's longest submarine channel, the Northwest Atlantic Mid-Ocean Channel, is found on a glaciated margin (Hesse et al., 1997). The Northwest Atlantic Mid-Ocean Channel extends for ~3800 km from the Labrador Sea (at water depths of <500 m) into the North Atlantic (at water depths >3500 m) (Hesse et al., 1997). The controls on submarine channel formation along glaciated margins are therefore even more uncertain than river-fed margins; but it is likely that these channels play a key role in sediment budgets, oceanography and ecosystems of glaciated margins (Powell and Domack, 1995; Hunter et al., 1996a; Bourgeois et al., 2016; Calleja et al., 2017).

Using detailed bathymetric mapping, submarine channels have been identified in contemporary fjord systems associated with river deltas and, at high latitudes, with marine-terminating outlet glaciers (Prior et al., 1987; Bornhold et al., 1994; Hughes Clarke et al., 2014; Batchelor et al., 2018). These datasets enable us to analyse and better understand the controls on channel formation and turbidity current recurrence in fjords with marine-terminating glaciers. An improved understanding of controls in fjords can also be applied to continental margins where ice previously reached the shelf edge, and thus help us to understand the evolution of these margins, their glacial histories, and their geohazard potential (L'Heureux et al., 2013; Gales et al., 2014; Newton and Huuse, 2017). It can also inform marine resource potential assessment related to turbidity current deposits (Syvitski and Farrow, 1989; Tasianas et al., 2016).

Where rivers discharge into fjords, the occurrence of turbidity currents is believed to be related to the pattern of glacier retreat. While glaciers provide large amounts of sediment, proglacial lakes can considerably hinder the supply of sediment to fjords (Normandeau et al., 2019). Where turbidity current occur, the formation of channels is thought to be related to the area of the river drainage basin and the highest mean annual discharges (Gales et al., 2019). Larger drainage basins are required in order for sufficient sediment to be supplied to river deltas (Gales et al., 2019). These elevated discharges concentrate deposition of this sediment during specific periods, resulting in the build-up of more unstable sediment due to its rapid deposition (Clare et al., 2016; Pope et al., 2017). The unstable nature of this sediment makes it more prone to failure and thus favours a greater number of turbidity currents thereby allowing channel incision to occur (Conway et al., 2012; Hughes Clarke et al., 2014; Clare et al., 2016; Hizzett et al., 2018; Gales et al., 2019). Alternatively, rivers discharging into fjords can transport sufficient sediment to result in the formation of hyperpycnal flows (Normark and Piper, 1991). Although rare, hyperpycnal flows have the potential to either incise channels or trigger turbidity currents that allow channel incision to occur (Normark and Piper, 1991; Conway et al., 2012).

In glaciated fjords, climatic regimes are often viewed as the primary control on the presence/absence of channels (Powell and Molnia, 1989; Syvitski, 1989; Syvitski and Shaw, 1995; Dowdeswell et al., 2016a; Batchelor et al., 2018), largely due to their perceived influence on sedimentation rates at the glacier terminus. Warmer climates are associated with higher rates of surface melt and therefore the availability of meltwater. Once at the bed, this meltwater can enhance sediment delivery to the terminus by increasing glacier velocity and flushing subglacial sediment through a channelized subglacial drainage system (Powell, 1991; Nienow et al., 1998; Cowan et al., 1999; Zwally et al., 2002; Tedesco et al., 2013). Higher rates of meltwater-derived sedimentation should favour the triggering of turbidity currents as a consequence of hyperpycnal flows or the rapid deposition of sediment (Mackiewicz et al., 1984; Carlson et al., 1989; Hunter et al., 1996a; Cowan et al., 1999; Clare et al., 2016). It is notable, however, that some fjords in the same climatic setting contain channels whilst

others do not (Batchelor et al., 2018). It is therefore clear that climate alone does not control channel formation in these settings.

Other glaciological and geological factors are also likely to have an impact in controlling the likelihood of channel formation in addition to climate. The size of the glacier drainage basin may determine the volume of sediment which could potentially be delivered to the terminus (Dowdeswell et al., 1996). Terminus stability may also control the supply of sediment to a given location, by determining the length of time for sediment to build up in any given location (Powell and Alley, 1997). Bedrock lithology and the thickness of subglacial till (if present) may also modulate the volume of sediment available for transport to the glacier terminus (Hallet, 1979; Hallet et al., 1996). Likewise, the slope gradient of the base of the fjord may also influence the likelihood of turbidity currents being triggered and their runout distance; low gradient and reverse slopes limiting turbidity current activity (Talling et al., 2013). This study investigates the relative roles of these controls for marine-terminating glacier-influenced, fjord systems in relation to potential climatic controls.

The key objectives of this study are to: 1) map and characterise turbidity current channels found offshore of northwest and southeast Greenland; (2) characterise the glacier catchments and fjords associated and not associated with channels and; (3) understand the controls on the formation (or absence) of submarine channels along glaciated margins.

2. Methods and Data

2.1. Bathymetry

The primary bathymetric dataset used in this study was acquired by NASA's Oceans Melting Greenland (OMG) project (Fenty et al., 2016; OMG Mission, 2016). This dataset was collected using a Teledyne Reson SeaBat 7160 Multibeam Echo Sounder, which has a frequency of 44 kHz and 512 beams. The OMG data are supplemented by bathymetric data from Rinks Fjord and the inner shelf of Uummannaq Trough, which were collected during the JR175 cruise of the RRS *James Clark Ross* in September 2009 (Ó Cofaigh et al., 2013). The JR175 cruise used a Kongsberg-Simrad EM120 system operating at 12 kHz

with 191 beams. The OMG and JR175 datasets were gridded using ArcGIS with a cell size of 25 m. These datasets (Figs 1 and 2) were used to analyse the presence/absence of submarine channels along the northwest and southeast Greenland margins, together with their morphology and the morphology of fjords along these margins. In the absence of clear definitions and criteria (Surpless et al., 2009) we distinguish submarine channels from gullies and chutes based on scale and morphology. Gullies and chutes are generally smaller, straighter and less incised especially in fjord environments (Field et al., 1999; Gales et al., 2019). Average channel slope gradients were extracted and averaged along channel thalwegs. Average fjord gradients were generated by averaging the slope gradients along fjord long profiles.

2.1.1. Alaskan bathymetry

Multibeam bathymetry of Endicott Arm, Glacier Bay and Behm Canal, Alaska were downloaded from NOAA's hydrographic survey database (https://maps.ngdc.noaa.gov/viewers/bathymetry). The datasets were collected during surveys of the NOAA vessels *Fairweather* in 2007 and 2009, and *Rainier* in 2013. The datasets were collected using RESON 7111, 7125, 8160 and 8101 multibeam echo sounders during the *Fairweather* cruises. Kongsberg EM710 and Reson 7125 echo sounders were used to collect bathymetry data onboard the *Rainier* in 2013. The datasets were gridded with cell sizes of 16 – 32 m depending on maximum water depth.

2.2. Satellite Imagery

Landsat 8 satellite imagery is used to show the modern margin of the Greenland Ice Sheet in our study areas. The satellite images acquired were from July to September 2015, 2016 and 2017. Images were selected based on the lowest percentage cloud cover available.

2.3. Drainage catchments and pathways

To assess the relationship between submarine channel presence and the approximate catchment size of the Greenlandic outlet glaciers we used local hydrostatic pressure fields to delineate the

hydrological catchments of each outlet glacier (e.g. Pattyn, 2010; Livingstone et al., 2013; Willis et al., 2016). To achieve this, we used the latest 150 m DEMs from BedMachine v3 of the surface and bed (Fig. 3a) of the Greenland Ice Sheet (Morlighem et al., 2017). The DEMs were used to calculate the subglacial hydrological potential (φ) and the major drainage catchments. φ was calculated from:

$$\varphi = \rho_i g z_s + (\rho_w - \rho_i) g z_b \quad (1)$$

where ρ_i = 910 kg m^{-3} is the density of ice, ρ_w = 1000 kg m^{-3} is the density of water, g = 9.8 m^{-2} is the acceleration due to gravity, z_s is the ice surface elevation, and z_b is the bed elevation (see Fig. 3b; Shreve, 1972). Sinks in the φ surface were identified and filled. The sink-filled φ was used to calculate the flow pathways and thus define the subglacial drainage basins beneath the Greenland Ice Sheet (Fig. 3c).

2.4. Ice flux

The contemporary ice flux at each glacier terminus was reconstructed using DEMs from the BedMachine v3 dataset and MEaSUREs Greenland Annual Ice Sheet Velocity Mosaics from InSAR and Landsat v2 (Joughin et al., 2015, updated 2017). This was achieved by multiplying the cross-sectional area of the ice front, derived from the BedMachine v3 dataset, with the depth-averaged velocity near the terminus based on surface velocity measurements using synthetic-aperture-radar interferometry (InSAR) and assuming basal velocity to be 80% of surface velocity (Overeem et al., 2017).

2.5. Surface runoff

To estimate the relative annual delivery of meltwater to each outlet glacier terminus we used the RACMO2.3 regional-atmospheric climate model (Noël et al., 2018). RACMO2.3 combines a high-resolution weather prediction model, and the European Centre for Medium-range Weather Forecasts, with advanced snow models to determine daily ice sheet surface mass balance (Ettema, Van den Broeke, Van Meijgaard and Van de Berg, 2010; Ettema, Van den Broeke, Van Meijgaard, Van de Berg, et al., 2010). We use RACMO2.3 monthly cumulative runoff output from 01/01/2008 to 31/12/2017

(Fig. 4). Runoff is defined as the sum of rain and melt, minus local refreezing and retention, and was calculated for the entire Greenland Ice Sheet at 1 km resolution. We overlayed the glacier catchments with the gridded RACMO2.3 data and summed the runoff for all grid cells for a given month and then averaged each individual month between 2008 and 2017. The average runoff is assumed to represent the monthly discharge from the subglacial drainage system at the terminus (Overeem et al., 2017).

2.6. Uncertainties

2.6.1. Submarine channel identification

It is probable that all large channels within the footprint of our bathymetry data have been identified. However, it is possible that smaller channels, i.e. shallow channels or those with widths <25 m, are not identified. In addition, the lengths of identified channels may be underreported. This is a consequence of the 25 m spatial resolution of the bathymetric datasets and their coarsening vertical resolution with increasing water depth, which may result in channels becoming indistinct from the seafloor.

2.6.2. Drainage catchments, pathways and ice fluxes

Our delineation of drainage catchments, pathways and ice fluxes contains a number of inherent uncertainties. These are a consequence of uncertainties in the BedMachine v3 ice thickness and bed elevation datasets resulting from the need to interpolate between radar lines and sources of error in the MEaSUREs dataset (see Morlighem et al., 2017 and Joughin et al. 2015). They are also a consequence of our decision to assume that basal velocities equate to 80% of surface velocities. However, our intention is to compare and contrast obvious differences between catchments rather than compare absolute values.

2.6.3. Surface runoff

Our methodology to estimate meltwater discharge incorporates a number of uncertainties. First, it assumes that runoff is transmitted straight to the bed and is not stored either in supraglacial lakes or

englacially (Banwell et al., 2012). However, a significant volume of meltwater may be prevented from reaching the ice margin because of refreezing and infiltration (Bamber et al., 2012; Harper et al., 2012). Second, we assume rapid and efficient transmission through the subglacial drainage system. However, the efficiency of the drainage system will vary over the year depending on surface meltwater inputs (Hewitt et al., 2012; Schoof et al., 2012; Hewitt, 2013) and meltwater may also be stored by subglacial lakes (Palmer et al., 2013). Nonetheless, we assume that the estimated runoff is a reasonable reflection of the relative subglacial discharge volumes of the individual catchments.

3. Results

3.1. Presence/absence of channels in fjords

The OMG and JR175 datasets contain bathymetry for 72 fjords and bathymetric troughs (i.e. troughs not bounded by aerially exposed margins) offshore of calving glacier margins which are sufficiently well mapped to identify the presence/absence of submarine channels (Figs 5 and 6, Tables 1 and 2). There are 35 fjords in northwest Greenland, 11 of which contain channels and 37 fjords in southeast Greenland, 23 of which contain submarine channels.

Where present in the fjords/troughs offshore of northwest Greenland, submarine channels are the dominant features on the otherwise relatively smooth fjord seafloor (Fig. 5). In contrast, where channels are not present the fjord bottom tends to be more rugged and the primary morphological features are elongate ridges, streamlined ridges, bedrock outcrops, fault scarps, knolls, low amplitude terraces or multiple small closely spaced moraines (Fig. 7; see Batchelor et al., 2018 for more details). Channel heads offshore of northwest Greenland are associated with either moraines or grounding-zone wedges (Fig. 5) but beyond these features the fjords slope gently into deeper water with average gradients of 2.2^{o} (min 1.67^{o}, max 3.17^{o}). In contrast, fjords without channels are far more variable. These fjords either lack comparably large moraines/grounding-zone wedges, exhibit a series of over-deepenings, or quickly become smooth-bottomed with extremely low gradients. Average fjord seafloor gradients and the boxplots in Fig. 8f illustrate this variability. The average slope gradient for

fjords which do not contain submarine channels is 4.33°, but the average gradient for individual fjords ranges from 1.1° to 12.2°. Furthermore, the gradient of fjords containing channels is statistically different from ones without channels at the 95% confidence interval (Table 3).

In contrast to northwest Greenland, the fjords of southeast Greenland are on average longer and narrower. The majority of these fjords can be characterised as a series of over-deepened basins often separated by moraines (Fig. 6c – d). Where fjords are separated into multiple basins, streamlined ridges and reverse slopes are often found. In southeast Greenland submarine channel heads are associated with moraines and occur where fjord gradients are relatively consistent (Fig. 6c, d). Channels terminate where the fjord seafloor becomes flat or the gradient is reversed and the seaward path is blocked by a moraine or bedrock sill (e.g. Fig. 5b and 6c). Channels do not form where gradients are extremely low (<1°) beyond a moraine/grounding-zone wedge, or where the fjord slope abruptly reverses (Figs 7 and 8f, Table 2). The difference between fjords is negligible and statistically insignificant ($p = 0.761$) when the dataset is considered as a whole. However, if two outliers are removed (Table 2; Timmiarmiit Kangertiva (4.82°) and Apuseeq (8.76°)), then the difference in the gradient of fjords associated with and not associated with channels is significant as the majority of those not associated with channels have gradients <1° (Fig. 8). The large gradients of Timmiarmiit Kangertiva Fjord and the fjord associated with Apusseeq Glacier are a consequence of a steep initial slope (averaging 7° for the first 4000 m) and a series of steep overdeepened basins, respectively.

3.2. Glacier catchments and ice fluxes

Glaciers draining into fjords/troughs represented in our data have catchment areas of between 27 km^2 and 55,000 km^2 (Tables 1 and 2). Overall, the average catchment area of those glaciers associated with channels and those not associated with channels are 8,300 km^2 and 2,900 km^2, respectively. In northwest Greenland the average catchment associated with a channel is 16,900 km^2, compared with 2,300 km^2 for those which are not (Fig. 8). In southeast Greenland the average catchment area for glaciers associated with channels is smaller (5,000 km^2) than in northwest Greenland but is still greater

than those catchments not associated with a channel (3,800 km^2). Overall, catchment size is a statistically significant factor (p = 0.048) in determining channel presence, but is insignificant in more localised datasets with fewer examples, i.e. in southeast Greenland alone (p = 0.68, Table 3).

The annual ice flux to the fjords/troughs in the datasets was between 5.8 x 10^{-5} $km^3\ a^{-1}$ and 24 $km^3\ a^{-1}$ (Fig. 8). As with catchment area, average ice discharge into fjords associated with channels was greater (2.87 $km^3\ a^{-1}$) than ice discharge into fjords not containing channels (2.39 $km^3\ a^{-1}$). In northwest Greenland, annual ice fluxes were considerably greater for catchments associated with submarine channels (3.44 $km^3\ a^{-1}$) than those not associated with channels (2.21 $km^3\ a^{-1}$). In southeast Greenland the relationship is similar but reflects the smaller contrasts in average catchment size (2.71 vs. 2.02 $km^3\ a^{-1}$). Unlike catchment area, differences in ice flux between catchments associated with channels and those which are not, is not statistically significant (Table 3).

3.3. Runoff

Glaciers which drained into fjords/troughs were modelled to have an average annual runoff between 0.003 $km^3\ a^{-1}$ and 0.44 $km^3\ a^{-1}$ from 2008 to 2017 (Fig. 8). The maximum monthly runoff varies between 0.001 $km^3\ a^{-1}$ and 0.22 $km^3\ a^{-1}$. The average for catchments associated with channels was greater (0.0838 $km^3\ a^{-1}$) than those without channels (0.072 $km^3\ a^{-1}$). A similar relationship exists for maximum monthly runoff (0.039 $km^3\ a^{-1}$ vs. 0.032 $km^3\ a^{-1}$). In northwest Greenland the average annual runoff was 0.066 $km^3\ a^{-1}$ per catchment, but those with channels had greater annual runoffs (0.13 $km^3\ a^{-1}$ vs. 0.046 $km^3\ a^{-1}$). Those with channels also had greater maximum monthly runoffs (Fig. 8; 0.069 $km^3\ a^{-1}$ vs. 0.022 $km^3\ a^{-1}$). Annual runoff and peak monthly runoff for catchments associated with channels were significantly greater than those without channels (see Table 3). In southeast Greenland the average runoff per catchment was greater than in northwest Greenland (0.081 $km^3 a^{-1}$), but the runoff for catchments associated with channels was lower than those without channels (0.068 $km^3\ a^{-1}$ vs. 0.11 $km^3\ a^{-1}$) as was their peak monthly runoff (0.027 $km^3\ a^{-1}$ vs. 0.048 $km^3\ a^{-1}$). The differences between annual runoff and peak monthly runoff of catchments associated and not associated with

channels were not significant in southeast Greenland or Greenland catchments as a whole although it was when considering only northwest Greenland.

3.4. Submarine channel dimensions/characteristics

Offshore of northwest and southeast Greenland, 37 submarine channels eroded into the seafloor have been identified (Figs 5 and 6; Table 1). Channel length and average width range from 2.2 km to 37.7 km and 62 m to 500 m respectively. Channel sinuosity ranges from 1.022 to 1.656. Of the 37 submarine channels, nine have well-developed terraces along at least part of their length (Fig. 5a – c). Knickpoints can be identified in some of the larger channels, e.g. Cornell, but crescentic shaped bedforms have not been identified although this may be a consequence of the resolution of the bathymetry data (typical 20 – 60 m crescent shaped bedforms would not be visible on a 25 m gridded bathymetric map). The presence of both knickpoints and crescentic shaped bedforms would be indicative of turbidity current activity (Wynn and Stow, 2002). Submarine channel knickpoints are normally characterised by anomalously steep sections of channel between which the mean slopes of the channel thalweg are either relatively constant or gradually decreasing (Mitchell, 2006). Periodic failure of knickpoints can result in the depth of the channel locally increasing as the knickpoint migrates up-channel, thus increasing channel entrenchment (Mitchell, 2006; Gales et al., 2019). In contrast, crescentic shaped bedforms are thought to be indicative of instabilities within sediment gravity flows resulting in zones of preferential erosion and deposition (Wynn and Stow, 2002; Symons et al., 2016).

Offshore of northwest Greenland there are 11 channels; offshore of southeast Greenland there are 26. Channels offshore of northwest and southeast Greenland are on average 14.9 km long and 8.5 km long respectively. Channels offshore of northwest Greenland are wider than those offshore of southeast Greenland (244 m vs. 137 m) and slightly more sinuous (1.2 vs. 1.16). Excluding the slope of the moraine/grounding-zone wedge on which channel heads originate, the average channel gradients for the two regions are 2.42° and 2.37° respectively. The average slope gradient where submarine

channels end is 0.7° with 75% of slope gradients between 0.52° and 0.92°. Offshore of northwest Greenland the average is 0.63° compared to 0.73° offshore of southeast Greenland.

Turbidity current channels can be broadly categorised into two types according to their length, widths and depths (Fig. 9; Table 4). Type 1 channels are less common (only 11 have been identified) and are found predominantly offshore of northwest Greenland. These channels are typically longer (5.7 – 37.7 km), wider (150 – 500 m) and deeper (10.5 – 46.3 m) than their type 2 counterparts (lengths 2.2 – 17.4 km; widths 61 – 321 m; depths 5 – 33.7). Indeed, type 1 channels are likely to be even more extensive as bathymetry does not cover the channel heads of the shortest or longest channels. In addition to the contrast in scale, type 1 channels also have well-developed terraces along at least part of their length, whereas no terraces are observed along type 2 channels. On average type 1 channels are slightly more sinuous than type 2 channels (1.18 vs. 1.17), although the range of type 2 channel sinuosities is greater (0.348 vs. 0.634). However, the difference in sinuosities is not statistically significant (Table 4).

4. Discussion

This section will initially discuss the controls on submarine channel formation offshore of northwest and southeast Greenland. General controls on channel presence are defined and compared to other regions where glaciers terminate in fjords and bathymetric troughs. It will then discuss the characteristics of the submarine channels within the dataset, and contrast these characteristics with those of submarine channels observed in other settings.

4.1. Controls on channel formation in fjords

4.1.1. Nature of seafloor substrate

The submarine channels identified in our bathymetric dataset are erosional landforms incised into the substrate, i.e. they have not been produced by the build-up of levees, and the channel floor is not perched above the surrounding seafloor (Peakall et al., 2000). Channels are only identified on

relatively smooth regions of the seafloor that are interpreted as sedimentary substrate (Figs. 5 and 6; Andrews et al., 1994; Schumann et al., 2012). This sedimentary substrate resulted from a combination of sedimentation from meltwater plumes, IRD, subglacial till formation and deposition related to mass movements (Powell, 2003). In contrast, no channel is found in a fjord where the seafloor is interpreted to be exposed bedrock, bedrock with a thin sedimentary drape, or where sediment has accumulated in the lee of obstacles (Fig. 7; Batchelor et al., 2018). This suggests that a sufficiently thick sedimentary substrate is required in a fjord for turbidity currents to be able to incise into the seabed and produce a submarine channel. Thus, a sufficiently deep sedimentary substrate appears to be a fundamental pre-requisite for channel formation since it indicates significant sediment delivery to the fjord.

4.1.2. Slope gradient

Differences in fjord gradient are a significant control on submarine channel formation (Table 3, Fig. 8). Fjords characterised by high seabed gradients (>3°) do not typically contain channels. These fjords often contain overdeepenings, multiple bedrock highs or reverse slopes (see Fig. 7). Typically, significant moraines or grounding-zone wedges are absent. In addition, fjords with very low average gradients do not contain submarine channels (Fig. 8). This is likely a consequence of low slope gradients controlling turbidity current flow dynamics (Normark and Piper, 1991). For example, flow on low gradients may be weak, and thus unable to incise the channel thalweg. Of the fjords of southeast Greenland where submarine channels are absent, 10 fjords have slope gradients of $\sim 1^{o}$. Even lower gradients (0.13 – 1.34^{o}) are found where submarine channels appear to terminate or, at the very least, become indistinguishable from the seafloor due to the resolution of our bathymetry. Initial acceleration of submarine mass movements is controlled by flow concentration, friction, and seabed gradient (Parker et al., 1986). Reducing slope angle will reduce both the number of turbidity currents triggered, as well as their acceleration. This will likely result in a reduction of the erosive potential of turbidity currents, and thus prevent channel incision (Kneller et al., 1999; Kneller and Buckee, 2000).

Slope breaks, such as those associated with the juncture between moraines and the fjord floor or between the main fjord and its tributary fjord, can also result in a rapid drop in turbidity current velocity (Mulder and Alexander, 2001). This can be a consequence of either the rapid reduction in slope gradient or as a result of rapid flow thickening due to the entrainment of seawater via strong mixing at the interface of the flow and the ambient water (Komar, 1971; Das et al., 2004). The rapid alteration of flow characteristics can reduce the flow capacity leading to rapid deposition and thus prevent any channel incision from occurring (Gray et al., 2005). Given these considerations it is perhaps unsurprising that the majority of submarine channels are found in fjords which have average slope gradients of between 1.6° and 2.9°, and that fjords with average gradients outside of this range constitute >75% of fjords which do not contain channels.

4.1.3. Stable glacier front

The primary glaciological control on submarine channel formation is the presence of a stable ice front. All submarine channel heads offshore of northwest and southeast Greenland are associated with moraines or grounding-zone wedges (Figs. 5 and 6). In northwest Greenland eight of the channels originate from moraines and grounding-zone wedges at or close to the modern glacier margin while three originate from former glacier margin positions. In southeast Greenland, only four are known to be associated with moraines and grounding-zone wedges associated with modern glacier positions. In this region, 14 are associated with features deposited when glaciers were more advanced and eight are unknown due to the channel heads existing beyond available bathymetry. Moraines and grounding-zone wedges are sedimentary depocentres formed by past and present glaciers and ice streams, when ice was present at that location for a significant period and/or was delivering sediment at a high rate (Ó Cofaigh et al., 2008; Batchelor and Dowdeswell, 2015). In the case of grounding-zone wedges, they are formed mainly through subglacial deposition of deforming till at the grounding-line but can be supplemented by meltwater-sedimentation and iceberg rainout (King et al., 1991; Powell and Alley, 1997). Subaqueous moraines form through deposition of till at the grounding-line, meltout,

meltwater-sedimentation, iceberg meltout and dumping (see e.g. Powell and Molnia, 1989). Both moraines and grounding-zone wedges may also record grounding-line oscillations which act to bulldoze and tectonise the sediments. The formation of a grounding-zone wedge is thought to typically be associated with the presence of a floating ice shelf at the glacier margin which can restrict vertical accommodation space immediately beyond the grounding zone (Powell and Domack, 1995; Batchelor and Dowdeswell, 2015); whilst moraines develop in the absence of an ice shelf (Ottesen et al., 2007; Batchelor and Dowdeswell, 2015). As a consequence of the contrasts in accommodation space, moraines typically have greater positive relief than grounding-zone wedges, in addition to lower length-to-height ratios (Dowdeswell and Fugelli, 2012). Once deposited, this material can subsequently be reworked by gravity-flow processes such as turbidity currents (Hunter et al., 1996a).

In general, moraine and grounding-zone wedge formation is controlled by: (1) grounding-zone stability (Larter and Vanneste, 1995; Ottesen et al., 2005); (2) accommodation space, i.e. the accommodation space of a tidewater terminating glacier will be greater than a glacier terminating in a floating ice shelf (King and Fader, 1986; Powell and Alley, 1997); (3) ice velocity and sedimentation rate (Dahlgren et al., 2002; Dowdeswell et al., 2008). Consistent delivery of sediment to these features from a stable ice front will increase the frequency of turbidity currents occurring. Growth of these features will also increase local slope gradients, favouring turbidity current triggering as a consequence of over-steepening (Clare et al., 2016). The likelihood of channel incision will therefore be enhanced.

4.1.4. Glacier catchment size, ice flux and runoff

If, as for rivers, the rate of sediment delivery controls the likelihood of channel formation one might hypothesise that catchment size, ice flux and runoff (meltwater discharge) should be correlated with the presence or absence of a channel (Hallet et al., 1996; Koppes et al., 2015; Overeem et al., 2017). Overall, our data suggests that larger glacier catchments and those with larger runoffs are more likely to be associated with submarine channels (Table 1, Fig. 8). However, the contrasts in the strengths of

the relationships which we observe between northwest and southeast Greenland suggest a more complex relationship, which we now discuss.

Northwest Greenland

Catchment size and ice flux might be expected to correlate with sediment delivery to the ice margin. This is a consequence of ice velocity being linked to rates of glacial erosion, and the area over which these processes operate (Hallet, 1996; Iverson, 2012; Koppes et al., 2015; Fernandez et al., 2016). In addition, large meltwater discharges can increase these rates of erosion through facilitating glacier sliding, and the flushing out of any sediment generated by other processes (Hooke and Elverhøi, 1996; Cuffey et al., 1999; Cowan et al., 2010; Boldt et al., 2013; Stokes, 2018). In northwest Greenland there is a statistical relationship between catchment size, runoff and peak monthly runoff and the presence of a submarine channels (Table 3; Fig. 8). Thus as catchment size and runoff increase, the likelihood of a submarine channel being present increases. These relationships are therefore similar to those hypothesised for rivers (Garrison et al., 1982; Babonneau et al., 2002; Pirmez and Imran, 2003; Schwenk et al., 2005). In contrast, although ice flux is greater for catchments where channels are present (Fig. 8) the difference is not statistically significant (Table 3). This may be a consequence of ice flux not directly correlating with sediment transport to the terminus due to other factors such as the nature of the subglacial bed, i.e. the presence/thickness of subglacial till. As a consequence, ice flux may not exert as much influence as catchment area or runoff volume in northwest Greenland.

Southeast Greenland

The number of submarine channels offshore of southeast Greenland is more than double that offshore of northwest Greenland, despite similar numbers of fjords being mapped in both regions (Table 1). This distribution supports the assertion that these features are more common in regions with warmer climates and thus more meltwater and sediment supply (Dowdeswell et al., 1998; Batchelor et al., 2018). This relationship is reflected in the average runoff for glaciers in southeast Greenland which exceed that for northwest Greenland glaciers (0.081 $km^3 a^{-1}$ vs. 0.066 $km^3 a^{-1}$).

As in northwest Greenland, catchments and ice fluxes associated with channels are greater on average than those not associated with channels, but the relationship with runoff is reversed (Fig. 8). In all cases the median values of catchments associated with channels are lower than those not associated with channels (Fig. 8). However, none of the variables are statistically different for catchments associated and not associated with submarine channels (Table 3). This illustrates the complex relationship between channel formation and ice flux and the possible role of other controls (see section 4.1.5).

We hypothesise that the weaker relationships between channel presence and catchment size, runoff and peak monthly runoff observed in northwest Greenland is a consequence of glacier retreat and thinning since the channels were last active. Out of 26 submarine channels that are known to be associated with moraines in southeast Greenland, 14 of the moraines have been abandoned following glacier retreat (Fig. 6). These channels are also not clearly defined on the bathymetry. Given that these channels are not well-defined and no longer directly connected to their sediment supply, we suggest that they are now inactive. The origin of an additional six channels is also unknown as they initiate beyond the current bathymetry coverage. In contrast, eight out of 11 moraines associated with channels are still associated with glacier termini in northwest Greenland and all of the channels appear to be currently active (Batchelor et al., 2018). We therefore suggest catchment areas, ice fluxes and runoff were likely greater when glaciers were in more advanced positions associated with the now abandoned moraines in southeast Greenland, which would make the relationships observed in northwest Greenland more widely applicable.

4.1.5. Other possible controls

Despite contrasts between the characteristics of catchments associated with and without submarine channels, a number of uncertainties remain. First, the volume of sediment exported by outlet glaciers in this study is likely influenced by the erodibility of their bedrock (Dühnforth et al., 2010). Currently, we have little to no information concerning the underlying geology of these glaciers, as only the

exposed bedrock in coastal regions is well known (Henriksen, 2009). This is further complicated by uncertainties around the processes of bedrock erosion, and the subsequent storage, transport and deposition of eroded material (Cowton et al., 2012). We are therefore uncertain as to the relative control of bedrock strength on rates of sediment transport, and thus its relative impacts on the likelihood of submarine channel formation.

Second, the thickness, deformability and thermal state (frozen/unfrozen) of basal till will impact the rate of sediment export by basal drag and meltwater flushing to the glacier terminus (Clarke, 1987; Iverson, 1991; Clark and Walder, 1994; Walder and Fowler, 1994; Hallet et al., 1996; Cuffey and Paterson, 2010). However, as with underlying geology, we have few direct measurements of the nature, extent and thickness of subglacial till for Greenland outlet glaciers. Our lack of understanding of subglacial till transport beneath the Greenland Ice Sheet represents a key uncertainty for understanding the presence/absence of submarine channels but also the role of ice sheets in global sediment budgets more generally (Jaeger and Koppes, 2016).

Third, it is possible that submarine channels exist or previously existed in some of the fjords which we have not identified. The bathymetry data does not extend to the glacier terminus in every fjord and it is possible that small submarine channels exist at the heads of some fjords. Seismic data in some fjords around Greenland (e.g. Kangerdlugssuaq Fjord; Syvitski et al., 1996) have also revealed the presence of buried submarine channels. However, no sub-bottom profiles or sediment cores were collected for the OMG project. It is therefore possible that a greater number of submarine channels existed around Greenland but they have since been buried by subsequent glacimarine and hemipelagic deposition.

4.2. Summary and general controls on channel presence

From our observations of submarine channels offshore of northwest and southeast Greenland, we propose a set of criteria controlling the likelihood that a channel will be present in a fjord containing a marine-terminating glacier (Fig. 10). First, larger glacier drainage areas increase the likelihood that a channel will be present, at least in northwest Greenland. Only one glacier with a drainage area <100

km^2 supplies sediment to a channel; only five are <200 km^2. Second, greater ice fluxes and runoff volumes increase the likelihood of submarine channel formation in northwest Greenland. However, these factors cannot contribute to channel formation if glacier terminuses are not stable. Therefore, the third factor is that the marine-terminating glacier terminus must be stable and deliver sufficient sediment for a moraine or grounding-zone wedge to form. Fourth, fjord/trough gradient should be consistent, between 1.5° and 3°, and slope seaward. Overdeepenings, very steep or shallow slopes will prevent channel formation. Fifth, fjords should initially contain sufficient sedimentary substrate to allow incision, which is dependent on previous controls over sediment supply.

4.3. Controls on turbidity current channel morphology

Turbidity current channel characteristics have been shown to be highly variable offshore of Greenland and have been categorised into two groups (see Section 3.4). However, whilst differences between the channels exist, we argue that this is not the result of fundamental contrasts in formational processes, but is more reflective of the frequency and power of turbidity currents in type 1 channels and the characteristics of catchments which supply them with sediment.

The contrasts in channel morphology are likely a consequence of the frequency and flow dynamics of turbidity currents in each system and therefore reflect differences in sediment delivery. Larger channels are likely to be a consequence of more frequent and more voluminous turbidity currents, which are more erosive. These flow characteristics would allow larger channels to form and be maintained (Klaucke and Hesse, 1996; Peakall et al., 2000; Hansen et al., 2017), and contrasts between turbidity current volumes would explain the formation of the channel terraces (Hagen et al., 1994). This is a consequence of channel terraces being a consequence of lower volume flows progressively filling the larger channel incised by larger flows (Hagen et al., 1994; Piper et al., 1999). An alternative mechanism of terrace formation has been proposed when terraces are a consequence of slumping of the channel sidewalls (Kenyon et al., 1995). Slumping has been observed on channel sidewalls but does not appear to be widespread. However, this interpretation would still favour the incision of larger

channels by more powerful turbidity currents. Unfortunately, we are unable to clearly identify a formative mechanism without seismic data across the terraces. Channels with similar morphologies to those identified as type 1 channels in this study have been identified offshore rivers that terminate in fjords (Conway et al., 2012). In the fluvial systems, the presence and size of channels has been linked to drainage basin size and river mean annual discharge as a consequence of their links with sediment delivery (Gales et al., 2019). However, our data suggests that while the larger type 1 channels are associated with larger catchments, greater annual and peak runoff, none of these factors are statistically significant in terms of explaining channel morphology (Table 4). Nevertheless, a greater proportion of type 2 channels are associated with moraines which have been abandoned by their outlet glaciers, and thus inputs may have been greater when channels were still active. It is therefore difficult to attribute the development of different channel morphologies to either the rate of sediment delivery or the mechanism by which it is delivered, i.e. meltwater or subglacial till transport, without direct measurements at the glacier margins.

Other possible controls on channel morphology in glacier-fed systems include glacier front stability, fjord gradient and concentrated or distributed sediment delivery. Delivery of glacigenic sediment to a single location over a longer period of time is likely to favour the formation of a type 1 channel. Consistent slope gradient over large distances also favours type 1 channel formation as turbidity current characteristics are not altered by changes in slope gradient (Peakall et al., 2000). We can see in the bathymetry data (Fig. 5) that channels rapidly terminate where the fjord becomes flat bottomed. The mean seafloor gradient where channels terminate in northwest and southeast Greenland is 0.72° (min 0.13°, max 1.34°). Low slope gradients therefore clearly limit channel development. A concentrated sediment delivery system (i.e. concentrated over specific sections of the glacier front) may also favour type 1 channel formation. This is a consequence of higher sedimentation rates favouring the triggering of turbidity currents. However, without repeat high-resolution bathymetry close to the glacier front it is difficult to test whether different glaciers favour specific regimes. This is especially true where moraines have been abandoned by their glacier.

4.4. Do controls on channel formation in Greenland apply to other glaciated regions?

4.4.1. Alaska

Alaskan tidewater glaciers are commonly associated with submarine channels due to the high meltwater and sediment fluxes that characterise glaciers in this region (Powell and Molnia, 1989; Powell, 1990; Powell and Domack, 1995; Hunter et al., 1996a, b; Cowan et al., 1997; Cowan et al., 1999; Cowan et al., 2010). Of the nine fjords into which tidewater glaciers terminate where high resolution bathymetry is available; four contain submarine channels (Table 5; Fig. 11a, b). Submarine bedforms formed as a consequence of turbidity currents are also present on the ice-contact fan delta associated with the Lamplugh Glacier, and an extensive submarine channel system is present offshore of the glaciofluvial delta associated with Carroll and Muir glaciers. There are also submarine channels associated with moraines which have been abandoned in Endicott Arm (Fig. 11c).

Applying our criteria governing the likelihood of submarine channel formation, we can see that active submarine channels in Alaska are associated with glaciers that have larger catchment sizes and high annual ice fluxes (Table 4). The channels are also found in fjords with moraines, consistent seaward sloping gradients and sufficient sediment to allow channel incision to occur (Fig. 11). In contrast, the heads of fjords which do not contain channels, with the exception of the Hubbard Glacier, have smaller catchment areas as well as flat bottoms as a consequence of sediment filled overdeepenings. Submarine channels or large chutes are present in the outer parts of Northwestern Bay, Aialik Bay and Resurrection Bay but these are all associated with moraines when glaciers had advanced much further than at present.

4.4.2. Svalbard

Svalbard has a cooler climate than South Alaska or South Georgia (next section) (Dowdeswell et al., 2016b), thereby reducing the likelihood of channel formation as a consequence of lower melt production. Here, high resolution bathymetry has been published for 30 fjords and outlets (Ottesen and Dowdeswell, 2006, 2009; Ottesen et al., 2008, 2017; Baeten et al., 2010; Forwick et al., 2010,

2016; Robinson and Dowdeswell, 2011; Kempf et al., 2013; Hansen, 2014; Burton et al., 2016a, b; Farnsworth et al., 2017; Flink et al., 2017, 2018; Streuff et al., 2017, 2018; Leister, 2018). These fjords and outlets are commonly characterised by terminal moraines associated with previous glacier surges, retreat moraines, lineations, elongated streamlined features, eskers and subglacial meltwater channels (Table 6). However, there is no evidence that submarine channels associated with marine-terminating glaciers are present. There are a number of possible explanations for this that are related to the surge-type nature of many of the glaciers and the local geometry of the fjords and outlets. First, a large number of glaciers for which we have offshore bathymetry are known or are thought to be surge-type glaciers (Hagen et al., 1993; Jiskoot et al., 2000). Surges from these glaciers have led to the deposition of low gradient (in planform) terminal moraines. Despite the more erodible preglacial bedrock of Svalbard compared to East Greenland (Solheim et al., 1998), the only additional moraines are small retreat moraines, and these are only found in some catchments. In other catchments, additional moraines are absent. This suggests that either the glacier fronts did not remain stationary during retreat for a sufficiently long period to build up larger moraines or that sediment volumes delivered to the glacier terminus during its quiescent phase were low (Ottesen and Dowdeswell, 2009). Second, the average catchment size and ice flux of glaciers terminating in these fjords is an order of magnitude and two orders of magnitude smaller, respectively, than the Greenland catchments associated with submarine channels (Table 1 and 6). Third, once seaward of the fjords, much of the submarine geomorphology suggests a divergent ice front and thus a more dispersed sedimentation regime. These factors would all reduce the likelihood of triggering the turbidity currents required for channel incision. Although turbidity current channels are not observed in Svalbard, many of the terminal moraines are associated with debris flow lobes, suggesting that this form of mass movement is more common.

4.4.3. South Georgia

South Georgia is situated between the Antarctic Peninsula and southernmost South America. High resolution bathymetry has been collected for the majority of the fjords on its northern side and two fjords on its southern side (Table 5; Hodgson et al., 2014). With the exception of a proglacial meltwater channel in Royal Bay (Hodgson et al., 2014), there is no evidence of submarine channels in any of the fjords. If considered in isolation, the bathymetry of Royal Bay, Cumberland Bay East, Cumberland Bay West and Drygalski Fjord favours the formation of submarine channels (Table 5) as they are characterised by sediment covered seafloors that slope seaward. However, the size of their drainage basins is limited (Table 5). This may suggest that, in these catchments, the supply of sediment to moraines or grounding-zone wedges is insufficient to result in frequent turbidity current occurrence, thus preventing submarine channel incision. In contrast, the seafloor of Stromness Bay and Husvik Bay is characterised by either multiple small moraines or exposed bedrock (Hodgson et al., 2014), neither of which favour the presence of submarine channels. Meanwhile Possession Bay and King Haakon Bay are dominated by overdeepened basins and low slope gradients on the inner continental shelf (Hodgson et al., 2014).

The examples above demonstrate that it is possible to use the general criteria outlined to predict the likelihood that a submarine channel will form in a glacially-influenced fjord. They support the assertion that warmer climates with abundant meltwater and meltwater sedimentation will favour the formation of submarine channels (Powell, 1990; Powell and Alley, 1997; Dowdeswell et al., 2016a). It is acknowledged, however, that there are additional local controls which are likely to add complexity, such as glacier type, local bedrock geology, and sediment characteristics.

5. Conclusions

Submarine channels are a common feature of the world's oceans, acting as conduits for the transport of material from coastal environment to the deep sea. However, the conditions that permit or prevent submarine channel formation are poorly understood. This is particularly true of glaciated environments. To understand the factors governing submarine channel formation in contemporary

glaciated environments, we present detailed bathymetric data from offshore of northwest and southeast Greenland to assess the controls on formation of submarine channels.

The bathymetry data revealed submarine channels in 34 out of 72 fjords. Channels were three times more numerous offshore southeast than northwest Greenland, likely reflecting the warmer climatic setting and the greater availability of meltwater. In northwest Greenland, submarine channels are associated with larger glacier catchments with greater runoff volumes. In southeast Greenland, these statistical relationships break down and are reversed in some cases (i.e. average annual runoff), but this is believed to partly be a consequence of channels being associated with abandoned moraines. Our estimates of ice discharge and meltwater runoff are therefore not reflective of the catchment when the glacier was in a more advanced position. We therefore propose that submarine channels are indeed more likely to form where catchments are larger and ice and meltwater fluxes are greater. However, the morphological characteristics of each fjord will also modulate whether a channel will form, i.e. is there sufficient sedimentary substrate and a consistent downslope gradient with few obstacles (Fig. 10). A thin or absent sedimentary substrate and highly variable slopes with reverse gradients will likely prevent channel formation. From this, we have proposed a series of criteria for predicting whether a submarine channel is likely to form in a fjord containing a marine-terminating glacier (Fig. 10). Observations from other settings such as Alaska, Svalbard and South Georgia appear to support these criteria. Further work on sediment delivery rates by different subglacial processes for tidewater terminating glaciers and characterisation of this sediment will help to better constrain the processes controlling channel formation, and the characteristics of turbidity currents in these environments.

The identified submarine channels have been categorised into two distinctive types based on statistical differences between their lengths, widths and depths. Variations in channel morphology according these criteria are likely to be a consequence of contrasting frequency and magnitude of turbidity currents within each system. They are less likely to be a consequence of fundamentally

different processes occurring in the different catchments. However, without any direct observations of turbidity currents in glaciated systems, future work should seek to explore whether contrasts in sediment grain size and delivery mechanism significantly impact upon turbidity current dynamics in these settings.

Acknowledgements

We thank NASA's Oceans Melting Greenland (OMG) project for access to the bathymetric data from northwest and southeast Greenland. Brice Noël is thanked for processing the RAMCO2.3 model and providing the runoff data. We are grateful to the US Geological Survey Earth Resources Observation Science Centre for providing Landsat imagery free of charge and the National Oceanic and Atmospheric Administration for making bathymetry from offshore of Alaska freely available. We thank Kelly Hogan for processing the JR175 data. E. Pope was supported by a Leverhulme Trust Early Career Fellowship (ECF-2018-267) and NERC grant NE/K011480/1.The bathymetric data that was collected during JR175 of the RRS *James Clark Ross* to West Greenland in 2009 was funded by Natural Environmental Research Council grant NE/D001951/1 to C. Ó Cofaigh. We would like to thank the editor Michele Rebesco, David Amblas, and an anonymous reviewer for their in depth reviews that improved this manuscript.

References

Amblas, D., Canals, M., Gerber, T.P., 2015. The long-term evolution of submarine canyons: insights from the NW Mediterranean. CIESM Monogr 47, 171-181.

Amblas, D., Ceramicola, S., Gerber, T.P., Canals, M., Chiocci, F.L., Dowdeswell, J.A., Harris, P.T., Huvenne, V.A.I., Lai, S.Y.J., Lastras, G., Lo Iacono, C., Micallef, A., Mountjoy, J.J., Paull, C.K., Puig, P., Sanchez-Vidal, A., 2018. Submarine Canyons and Gullies, in: Micallef, A., Krastel, S., Savini, A. (Eds.), Submarine Geomorphology. Springer International Publishing, Cham, pp. 251-272.

Andrews, J.T., Milliman, J.D., Jennings, A.E., Rynes, N., Dwyer, J., 1994. Sediment thicknesses and Holocene glacial marine sedimentation rates in three East Greenland fjords (ca. 68 N). The Journal of Geology 102, 669-683.

Azpiroz-Zabala, M., Cartigny, M.J.B., Talling, P.J., Parsons, D.R., Sumner, E.J., Clare, M.A., Simmons, S.M., Cooper, C., Pope, E.L., 2017. Newly recognised turbidity current structure can explain prolonged flushing of submarine canyons. Science Advances 3, e1700200.

Babonneau, N., Savoye, B., Cremer, M., Klein, B., 2002. Morphology and architecture of the present canyon and channel system of the Zaire deep-sea fan. Marine and Petroleum Geology 19, 445-467.

Baeten, N.J., Forwick, M., Vogt, C., Vorren, T.O., 2010. Late Weichselian and Holocene sedimentary environments and glacial activity in Billefjorden, Svalbard. Geological Society, London, Special Publications 344, 207-223.

Bamber, J.L., van den Broeke, M.R., Ettema, J., Lenaerts, J.T.M., Rignot, E., 2012. Recent large increases in freshwater fluxes from Greenland into the North Atlantic. Geophysical Research Letters 39, L19501.

Banwell, A.F., Arnold, N.S., Willis, I.C., Tedesco, M., Ahlstrøm, A.P., 2012. Modeling supraglacial water routing and lake filling on the Greenland Ice Sheet. Journal of Geophysical Research: Earth Surface 117, F04012.

Batchelor, C.L., Dowdeswell, J.A., 2015. Ice-sheet grounding-zone wedges (GZWs) on high-latitude continental margins. Marine Geology 363, 65-92.

Batchelor, C.L., Dowdeswell, J.A., Rignot, E., 2018. Submarine landforms reveal varying rates and styles of deglaciation in North-West Greenland fjords. Marine Geology 402, 60-80.

Bjørk, A.A., Kruse, L.M., Michaelsen, P.B., 2015. Brief communication: Getting Greenland's glaciers right–a new data set of all official Greenlandic glacier names. The Cryosphere 9, 2215-2218.

Boldt, K.V., Nittrouer, C.A., Hallet, B., Koppes, M.N., Forrest, B.K., Wellner, J.S., Anderson, J.B., 2013. Modern rates of glacial sediment accumulation along a 15° S-N transect in fjords from the Antarctic Peninsula to southern Chile. Journal of Geophysical Research: Earth Surface 118, 2072-2088.

Bornhold, B.D., Ren, P., Prior, D.B., 1994. High-frequency turbidity currents in British Columbia fjords. Geo-Marine Letters 14, 238-243.

Bourgeois, S., Kerhervé, P., Calleja, M.L., Many, G., Morata, N., 2016. Glacier inputs influence organic matter composition and prokaryotic distribution in a high Arctic fjord (Kongsfjorden, Svalbard). Journal of Marine Systems 164, 112-127.

Brown, C.S., Meier, M.F., Post, A., 1982. Calving speed of Alaska tidewater glaciers, with application to Columbia Glacier. Geological Survey Professional Paper 1258-C (1982), 13.

Burton, D.J., Dowdeswell, J.A., Hogan, K.A., Noormets, R., 2016a. Little Ice Age terminal and retreat moraines in Kollerfjorden, NW Spitsbergen. Geological Society, London, Memoirs 46, 71-72.

Burton, D.J., Dowdeswell, J.A., Hogan, K.A., Noormets, R., 2016b. Marginal fluctuations of a Svalbard surge-type tidewater glacier, Blomstrandbreen, since the Little Ice Age: a record of three surges. Arctic, Antarctic, and Alpine Research 48, 411-426.

Calleja, M.L., Kerhervé, P., Bourgeois, S., Kędra, M., Leynaert, A., Devred, E., Babin, M., Morata, N., 2017. Effects of increase glacier discharge on phytoplankton bloom dynamics and pelagic geochemistry in a high Arctic fjord. Progress in Oceanography 159, 195-210.

Canals, M., Puig, P., de Madron, X.D., Heussner, S., Palanques, A., Fabres, J., 2006. Flushing submarine canyons. Nature 444, 354-357.

Carlson, P.R., Powell, R.D., Rearic, D.M., 1989. Turbidity-current channels in Queen Inlet, Glacier Bay, Alaska. Canadian Journal of Earth Sciences 26, 807-820.

Clare, M.A., Hughes Clarke, J.E., Talling, P.J., Cartigny, M.J.B., Pratomo, D.G., 2016. Preconditioning and triggering of offshore slope failures and turbidity currents revealed by most detailed monitoring yet at a fjord-head delta. Earth and Planetary Science Letters 450, 208-220.

Clark, J.D., Kenyon, N.H., Pickering, K.T., 1992. Quantitative analysis of the geometry of submarine channels: implications for the classification of submarine fans. Geology 20, 633-636.

Clark, J.D., Pickering, K.T., 1996. Submarine channels: Process and architecture. Vallis Press, London.

Clark, P.U., Walder, J.S., 1994. Subglacial drainage, eskers, and deforming beds beneath the Laurentide and Eurasian ice sheets. Geological Society of America Bulletin 106, 304-314.

Clarke, G.K.C., 1987. Subglacial till: a physical framework for its properties and processes. Journal of Geophysical Research: Solid Earth 92, 9023-9036.

Conway, K.W., Barrie, J.V., Picard, K., Bornhold, B.D., 2012. Submarine channel evolution: active channels in fjords, British Columbia, Canada. Geo-Marine Letters 32, 301-312.

Cowan, E.A., Cai, J., Powell, R.D., Clark, J.D., Pitcher, J.N., 1997. Temperate glacimarine varves: an example from Disenchantment Bay, southern Alaska. Journal of Sedimentary Research 67, 536 - 549.

Cowan, E.A., Seramur, K.C., Cai, J., Powell, R.D., 1999. Cyclic sedimentation produced by fluctuations in meltwater discharge, tides and marine productivity in an Alaskan fjord. Sedimentology 46, 1109-1126.

Cowan, E.A., Seramur, K.C., Powell, R.D., Willems, B.A., Gulick, S.P.S., Jaeger, J.M., 2010. Fjords as temporary sediment traps: History of glacial erosion and deposition in Muir Inlet, Glacier Bay National Park, southeastern Alaska. GSA Bulletin 122, 1067-1080.

Cowton, T., Nienow, P.W., Bartholomew, I., Sole, A., Mair, D., 2012. Rapid erosion beneath the Greenland ice sheet. Geology 40, 343-346.

Cuffey, K.M., Conway, H., Hallet, B., Gades, A.M., Raymond, C.F., 1999. Interfacial water in polar glaciers and glacier sliding at− 17 C. Geophysical Research Letters 26, 751-754.

Cuffey, K.M., Paterson, W.S.B., 2010. The physics of glaciers. Academic Press.

Dahlgren, K.I.T., Vorren, T.O., Laberg, J.S., 2002. The role of grounding-line sediment supply in ice-sheet advances and growth on continental shelves: an example from the mid-Norwegian sector of the Fennoscandian ice sheet during the Saalian and Weichselian. Quaternary International 95, 25-33.

Das, H.S., Imran, J., Pirmez, C., Mohrig, D., 2004. Numerical modeling of flow and bed evolution in meandering submarine channels. Journal of Geophysical Research: Oceans 109.

Dowdeswell, J.A., Canals, M., Jakobsson, M., Todd, B.J., Dowdeswell, E.K., Hogan, K.A., 2016a. Atlas of submarine glacial landforms: Modern, Quaternary and Ancient. Geological Society of London, pp. 519-552.

Dowdeswell, J.A., Canals, M., Jakobsson, M., Todd, B.J., Dowdeswell, E.K., Hogan, K.A., 2016b. Introduction: an Atlas of Submarine Glacial Landforms. Geological Society, London, Memoirs 46, 3-14.

Dowdeswell, J.A., Elverhoi, A., Spielhagen, R., 1998. Glacimarine sedimentary processes and facies on the Polar North Atlantic margins. Quaternary Science Reviews 17, 243-272.

Dowdeswell, J.A., Fugelli, E.M.G., 2012. The seismic architecture and geometry of grounding-zone wedges formed at the marine margins of past ice sheets. Bulletin 124, 1750-1761.

Dowdeswell, J.A., Kenyon, N.H., Elverhøi, A., Laberg, J.S., Hollender, F.J., Mienert, J., Siegert, M.J., 1996. Large-scale sedimentation on the glacier-influenced polar North Atlantic Margins: Long-range side-scan sonar evidence. Geophysical Research Letters 23, 3535-3538.

Dowdeswell, J.A., Ottesen, D., Evans, J., Ó Cofaigh, C., Anderson, J.B., 2008. Submarine glacial landforms and rates of ice-stream collapse. Geology 36, 819-822.

Dühnforth, M., Anderson, R.S., Ward, D., Stock, G.M., 2010. Bedrock fracture control of glacial erosion processes and rates. Geology 38, 423-426.

Ettema, J., Van den Broeke, M.R., Van Meijgaard, E., Van de Berg, W.J., 2010. Climate of the Greenland ice sheet using a high-resolution climate model-Part 2: Near-surface climate and energy balance. The Cryosphere 4, 529-544.

Ettema, J., Van den Broeke, M.R., Van Meijgaard, E., Van de Berg, W.J., Box, J.E., Steffen, K., 2010. Climate of the Greenland ice sheet using a high-resolution climate model-Part 1: Evaluation. The Cryosphere 4, 511-527.

Farnsworth, W.R., Ingólfsson, Ó., Noormets, R., Allaart, L., Alexanderson, H., Henriksen, M., Schomacker, A., 2017. Dynamic Holocene glacial history of St. Jonsfjorden, Svalbard. Boreas 46, 585-603.

Fenty, I., Willis, J.K., Khazendar, A., Dinardo, S., Forsberg, R., Fukumori, I., Holland, D.M., Jakobsson, M., Moller, D., Morison, J., 2016. Oceans Melting Greenland: Early results from NASA's ocean-ice mission in Greenland. Oceanography 29, 72-83.

Fernandez, R.A., Anderson, J.B., Wellner, J.S., Minzoni, R.L., Hallet, B., Smith, R.T., 2016. Latitudinal variation in glacial erosion rates from Patagonia and the Antarctic Peninsula (46 S–65 S). Bulletin 128, 1000-1023.

Field, M.E., Gardner, J.V., Prior, D.B., 1999. Geometry and significance of stacked gullies on the northern California slope. Marine Geology 154, 271-286.

Flink, A.E., Hill, P., Noormets, R., Kirchner, N., 2018. Holocene glacial evolution of Mohnbukta in eastern Spitsbergen. Boreas 47, 390-409.

Flink, A.E., Noormets, R., Fransner, O., Hogan, K.A., ÓRegan, M., Jakobsson, M., 2017. Past ice flow in Wahlenbergfjorden and its implications for late Quaternary ice sheet dynamics in northeastern Svalbard. Quaternary Science Reviews 163, 162-179.

Forwick, M., Dowdeswell, J.A., Laberg, J.S., Ottesen, D., 2016. Glacial landform assemblages in Spitsbergen fjords from the last full-glacial, deglaciation and the late Holocene. Geological Society, London, Memoirs 46, 147-150.

Forwick, M., Vorren, T.O., Hald, M., Korsun, S., Roh, Y., Vogt, C., Yoo, K.-C., 2010. Spatial and temporal influence of glaciers and rivers on the sedimentary environment in Sassenfjorden and Tempelfjorden, Spitsbergen. Geological Society, London, Special Publications 344, 163-193.

Gales, J.A., Leat, P.T., Larter, R.D., Kuhn, G., Hillenbrand, C.-D., Graham, A.G.C., Mitchell, N.C., Tate, A.J., Buys, G.B., Jokat, W., 2014. Large-scale submarine landslides, channel and gully systems on the southern Weddell Sea margin, Antarctica. Marine Geology 348, 73-87.

Gales, J.A., Talling, P.J., Cartigny, M.J.B., Hughes Clarke, J., Lintern, G., C., S., Clare, M.A., 2019. What controls submarine channel development and the morphology of deltas entering deep-water fjords? Earth Surface Processes and Landforms 44, 535-551.

Galy, V., France-Lanord, C., Beyssac, O., Faure, P., Kudrass, H., Palhol, F., 2007. Efficient organic carbon burial in the Bengal fan sustained by the Himalayan erosional system. Nature 450, 407-410.

Garrison, L.E., Kenyon, N.H., Bouma, A.H., 1982. Channel systems and lobe construction in the Mississippi Fan. Geo-Marine Letters 2, 31-39.

Goff, J.A., Lawson, D.E., Willems, B.A., Davis, M., Gulick, S.P.S., 2012. Morainal bank progradation and sediment accumulation in Disenchantment Bay, Alaska: Response to advancing Hubbard Glacier. Journal of Geophysical Research: Earth Surface 117, 1-15.

Gordon, J.E., Haynes, V.M., Hubbard, A., 2008. Recent glacier changes and climate trends on South Georgia. Global and Planetary Change 60, 72-84.

Gray, T.E., Alexander, J., Leeder, M.R., 2005. Quantifying velocity and turbulence structure in depositing sustained turbidity currents across breaks in slope. Sedimentology 52, 467-488.

Hagen, J.O., Liestøl, O., Roland, E., Jørgensen, T., 1993. Glacier atlas of Svalbard and Jan Mayen.

Hagen, R.A., Bergersen, D.D., Moberly, R., Coulbourn, W.T., 1994. Morphology of a large meandering submarine canyon system on the Peru-Chile forearc. Marine Geology 119, 7-38.

Hallet, B., 1979. A theoretical model of glacial abrasion. Journal of Glaciology 23, 39-50.

Hallet, B., 1996. Glacial quarrying: A simple theoretical model. Annals of Glaciology 22, 1-8.

Hallet, B., Hunter, L., Bogen, J., 1996. Rates of erosion and sediment evacuation by glaciers: A review of field data and their implications. Global and Planetary Change 12, 213-235.

Hansen, L., Janocko, M., Kane, I., Kneller, B., 2017. Submarine channel evolution, terrace development, and preservation of intra-channel thin-bedded turbidites: Mahin and Avon channels, offshore Nigeria. Marine Geology 383, 146-167.

Hansen, T., 2014. Late Weichselian and Holocene sedimentary processes and glacier dynamics in Woodfjorden, Bockfjorden and Liefdefjorden, North Spitsbergen. The Arctic University of Norway.

Harper, J., Humphrey, N., Pfeffer, W.T., Brown, J., Fettweis, X., 2012. Greenland ice-sheet contribution to sea-level rise buffered by meltwater storage in firn. Nature 491, 240-243.

Henriksen, N., 2009. Greenland from Archaean to Quaternary: Descriptive Text to the 1995 Geological Map of Greenland 1: 2 5000 000. Geological Survey of Denmark and Greenland, Ministry of Climate and Energy.

Hesse, R., Klaucke, I., Khodabakhsh, S., Ryan, W.B.F., 1997. Glacimarine Drainage Systems in Deep-sea: The NAMOC System of the Labrador Sea and its Sibling, in: Davies, T.A., al., e. (Eds.), Glaciated Continental Margins. Springer, pp. 286-289.

Hewitt, I.J., 2013. Seasonal changes in ice sheet motion due to melt water lubrication. Earth and Planetary Science Letters 371, 16-25.

Hewitt, I.J., Schoof, C.G., Werder, M.A., 2012. Flotation and free surface flow in a model for subglacial drainage. Part 2. Channel flow. Journal of Fluid Mechanics 702, 157-187.

Hizzett, J.L., Hughes Clarke, J.E., Sumner, E.J., Cartigny, M.J.B., Talling, P.J., Clare, M.A., 2018. Which Triggers Produce the Most Erosive, Frequent, and Longest Runout Turbidity Currents on Deltas? Geophysical Research Letters 45, 855-863.

Hodgson, D.A., Graham, A.G.C., Griffiths, H.J., Roberts, S.J., Ó Cofaigh, C., Bentley, M.J., Evans, D.J.A., 2014. Glacial history of sub-Antarctic South Georgia based on the submarine geomorphology of its fjords. Quaternary Science Reviews 89, 129-147.

Hooke, R.L.B., Elverhøi, A., 1996. Sediment flux from a fjord during glacial periods, Isfjorden, Spitsbergen. Global and Planetary Change 12, 237-249.

Hughes Clarke, J.E., Marques, C.R.V., Pratomo, D., 2014. Imaging Active Mass-Wasting and Sediment Flows on a Fjord Delta, Squamish, British Columbia, Submarine Mass Movements and Their Consequences. Springer, pp. 249-260.

Hunter, L.E., Powell, R.D., Lawson, D.E., 1996a. Morainal-bank sediment budgets and their influence on the stability of tidewater termini of valley glaciers entering Glacier Bay, Alaska, USA. Annals of Glaciology 22, 211-216.

Hunter, L.E., Powell, R.D., Smith, G.W., 1996b. Facies architecture and grounding-line fan processes of morainal banks during the deglaciation of coastal Maine. Geological Society of America Bulletin 108, 1022-1038.

Iverson, N.R., 1991. Morphology of glacial striae: implications for abrasion of glacier beds and fault surfaces. Geological Society of America Bulletin 103, 1308-1316.

Iverson, N.R., 2012. A theory of glacial quarrying for landscape evolution models. Geology 40, 679-682.

Jaeger, J.M., Koppes, M.N., 2016. The role of the cryosphere in source-to-sink systems. Earth-Science Reviews 153, 43-76.

Jakobsson, M., Mayer, L., Coakley, B., Dowdeswell, J.A., Forbes, S., Fridman, B., Hodnesdal, H., Noormets, R., Pedersen, R., Rebesco, M., 2012. The international bathymetric chart of the Arctic Ocean (IBCAO) version 3.0. Geophysical Research Letters 39, L12609.

Jiskoot, H., Murray, T., Boyle, P., 2000. Controls on the distribution of surge-type glaciers in Svalbard. Journal of Glaciology 46, 412-422.

Joughin, I., Smith, B., Howat, I., Scambos, T.A., 2015, updated 2017. *MEaSUREs Greenland Ice Sheet Velocity Map from InSAR Data, Version 2 (2016 - 2017)*. NASA National Snow and Ice Data Center Distributed Active Archive Center, Boulder, Colorado USA.

Kao, S.-J., Dai, M., Selvaraj, K., Zhai, W., Cai, P., Chen, S.-N., Yang, J.Y.T., Liu, J.T., Liu, C.C., Syvitski, J.P.M., 2010. Cyclone-driven deep sea injection of freshwater and heat by hyperpycnal flow in the subtropics. Geophysical Research Letters 37, L21702.

Kempf, P., Forwick, M., Laberg, J.S., Vorren, T.O., 2013. Late Weichselian and Holocene sedimentary palaeoenvironment and glacial activity in the high-arctic van Keulenfjorden, Spitsbergen. The Holocene 23, 1607-1618.

Kenyon, N.H., Amir, A., Cramp, A., 1995. Geometry of the younger sediment bodies of the Indus Fan, in: Pickering, K.T., Hiscott, R.N., Kenyon, N.H., Lucchi, R.F., Smith, R.D.A. (Eds.), Atlas of Deep Water Environments. Springer, Dordrecht, pp. 89-93.

King, L.H., Fader, G.B., 1986. Wisconsinan glaciation of the Atlantic continental shelf of southeast Canada. Geological Survey of Canada.

King, L.H., Rokoengen, K., Fader, G.B.J., Gunleiksrud, T., 1991. Till-tongue stratigraphy. Geological Society of America Bulletin 103, 637-659.

Klaucke, I., Hesse, R., 1996. Fluvial features in the deep-sea: new insights from the glacigenic submarine drainage system of the Northwest Atlantic Mid-Ocean Channel in the Labrador Sea. Sedimentary Geology 106, 223-234.

Kneller, B., 2003. The influence of flow parameters on turbidite slope channel architecture. Marine and Petroleum Geology 20, 901-910.

Kneller, B., Buckee, C., 2000. The structure and fluid mechanics of turbidity currents: a review of some recent studies and their geological implications. Sedimentology 47, 62-94.

Kneller, B.C., Bennett, S.J., McCaffrey, W.D., 1999. Velocity structure, turbulence and fluid stresses in experimental gravity currents. Journal of Geophysical Research: Oceans 104, 5381-5391.

Komar, P.D., 1971. Hydraulic jumps in turbidity currents. Geological Society of America Bulletin 82, 1477-1488.

Konsoer, K., Zinger, J., Parker, G., 2013. Bankfull hydraulic geometry of submarine channels created by turbidity currents: relations between bankfull channel characteristics and formative flow discharge. Journal of Geophysical Research: Earth Surface 118, 216-228.

Koppes, M., Hallet, B., Rignot, E., Mouginot, J., Wellner, J.S., Boldt, K., 2015. Observed latitudinal variations in erosion as a function of glacier dynamics. Nature 526, 100-103.

L'Heureux, J.S., Vanneste, M., Rise, L., Brendryen, J., Forsberg, C.F., Nadim, F., Longva, O., Chand, S., Kvalstad, T.J., Haflidason, H., 2013. Stability, mobility and failure mechanism for landslides at the upper continental slope off Vesterålen, Norway. Marine Geology 346, 192-207.

Lane, S.N., Richards, K.S., 1997. Linking river channel form and process: time, space and causality revisited. Earth Surface Processes and Landforms: The Journal of the British Geomorphological Group 22, 249-260.

Larter, R.D., Vanneste, L.E., 1995. Relict subglacial deltas on the Antarctic Peninsula outer shelf. Geology 23, 33-36.

Lastras, G., Arzola, R.G., Masson, D.G., Wynn, R.B., Huvenne, V.A.I., Hühnerbach, V., Canals, M., 2009. Geomorphology and sedimentary features in the Central Portuguese submarine canyons, Western Iberian margin. Geomorphology 103, 310-329.

Leister, J., 2018. Holocene Glacial Dynamics of the Barentsøya ice cap, Svalbard. UiT Norges arktiske universitet.

Leopold, L.B., Wolman, M.G., 1957. River channel patterns: braided, meandering, and straight. US Government Printing Office.

Livingstone, S., Clark, C.D., Woodward, J., Kingslake, J., 2013. Potential subglacial lake locations and meltwater drainage pathways beneath the Antarctic and Greenland ice sheets. Cryosphere 7, 1721-1740.

Mackiewicz, N.E., Powell, R.D., Carlson, P.R., Molnia, B.F., 1984. Interlaminated ice-proximal glacimarine sediments in Muir Inlet, Alaska. Marine Geology 57, 113-147.

Mitchell, N.C., 2005. Interpreting long-profiles of canyons in the USA Atlantic continental slope. Marine Geology 214, 75-99.

Mitchell, N.C., 2006. Morphologies of knickpoints in submarine canyons. Geological Society of America Bulletin 118, 589-605.

Morlighem, M., Williams, C.N., Rignot, E., An, L., Arndt, J.E., Bamber, J.L., Catania, G., Chauché, N., Dowdeswell, J.A., Dorschel, B., Fenty, I., Hogan, K., Howat, I., Hubbard, A., Jakobsson, M., Jordan, T.M., Kjeldsen, K.K., Millan, R., Mayer, L., Mouginot, J., Noël, B.P.Y., O'Cofaigh, C., Palmer, S., Rysgaard, S.,

Seroussi, H., Siegert, M.J., Slabon, P., Straneo, F., van den Broeke, M.R., Weinrebe, W., Wood, M., Zinglersen, K.B., 2017. BedMachine v3: Complete Bed Topography and Ocean Bathymetry Mapping of Greenland From Multibeam Echo Sounding Combined With Mass Conservation. Geophysical Research Letters 44, 10051-11061.

Mouginot, J., Rignot, E., Scheuchl, B., Millan, R., 2017. Comprehensive annual ice sheet velocity mapping using Landsat-8, Sentinel-1, and RADARSAT-2 data. Remote Sensing 9, 364.

Mulder, T., Alexander, J., 2001. Abrupt change in slope causes variation in the deposit thickness of concentrated particle-driven density currents. Marine Geology 175, 221-235.

Newton, A.M.W., Huuse, M., 2017. Late Cenozoic environmental changes along the Norwegian margin. Marine Geology 393, 216-244.

Nienow, P.W., Sharp, M.J., Willis, I.C., 1998. Seasonal changes in the morphology of the subglacial drainage system, Haut Glacier d'Arolla, Switzerland. Earth Surface Processes and Landforms: The Journal of the British Geomorphological Group 23, 825-843.

Noël, B., van de Berg, W.J., Wessem, V., Melchior, J., Van Meijgaard, E., Van As, D., Lenaerts, J.T.M., Lhermitte, S., Munneke, P.K., Smeets, C.J.P., 2018. Modelling the climate and surface mass balance of polar ice sheets using RACMO2-Part 1: Greenland (1958-2016). Cryosphere 12, 811-831.

Normandeau, A., Dietrich, P., Hughes Clarke, J.E., Van Wychen, W., Lajeunesse, P., Burgess, D., F., G.J., 2019. Retreat patterns of glaciers controls the occurrence of turbidity currents in high-laitude fjord deltas (eastern Baffin Island). Journal of Geophysical Research: Earth Surface. doi:10.1029/2018JF004970.

Normark, W.R., Piper, D.J.W., 1991. Initiation processes and flow evolution of turbidity currents: implications for the depositional record. SEPM Special Publications 46, 207-230.

Ó Cofaigh, C., Andrews, J.T., Jennings, A.E., Dowdeswell, J.A., Hogan, K.A., Kilfeather, A.A., Sheldon, C., 2013. Glacimarine lithofacies, provenance and depositional processes on a West Greenland trough-mouth fan. Journal of Quaternary Science 28, 13-26.

Ó Cofaigh, C., Dowdeswell, J.A., Evans, J., Kenyon, N.H., Taylor, J., Mienert, J., Wilken, M., 2004. Timing and significance of glacially influenced mass-wasting in the submarine channels of the Greenland Basin. Marine Geology 207, 39-54.

Ó Cofaigh, C., Dowdeswell, J.A., Evans, J., Larter, R.D., 2008. Geological constraints on Antarctic palaeo-ice-stream retreat. Earth Surface Processes and Landforms 33, 513-525.

Ó Cofaigh, C., Dowdeswell, J.A., Kenyon, N.H., 2006. Geophysical investigations of a high-latitude submarine channel system and associated channel-mouth lobe in the Lofoten Basin, polar North Atlantic. Marine Geology 226, 41-50.

Ó Cofaigh, C., Hogan, K.A., Jennings, A.E., Callard, S.L., Dowdeswell, J.A., Noormets, R., Evans, J., 2018. The role of meltwater in high-latitude trough-mouth fan development: The Disko Trough-Mouth Fan, West Greenland. Marine Geology 402, 17-32.

OMG. 2016. Bathymetry (sea floor depth) data from the ship-based bathymetry survey. Ver. 0.1. OMG SDS, California, USA, data set accessed August 6, 2018, at https://doi.org/10.5067/OMGEV-BTYSS.

Ottesen, D., Dowdeswell, J.A., 2006. Assemblages of submarine landforms produced by tidewater glaciers in Svalbard. Journal of Geophysical Research: Earth Surface (2003–2012) 111.

Ottesen, D., Dowdeswell, J.A., 2009. An inter–ice-stream glaciated margin: Submarine landforms and a geomorphic model based on marine-geophysical data from Svalbard. Geological Society of America Bulletin 121, 1647-1665.

Ottesen, D., Dowdeswell, J.A., Bellec, V.K., Bjarnadóttir, L.R., 2017. The geomorphic imprint of glacier surges into open-marine waters: examples from eastern Svalbard. Marine Geology 392, 1-29.

Ottesen, D., Dowdeswell, J.A., Benn, D.I., Kristensen, L., Christiansen, H.H., Christensen, O., Hansen, L., Lebesbye, E., Forwick, M., Vorren, T.O., 2008. Submarine landforms characteristic of glacier surges in two Spitsbergen fjords. Quaternary Science Reviews 27, 1583-1599.

Ottesen, D., Dowdeswell, J.A., Landvik, J.Y., Mienert, J., 2007. Dynamics of the Late Weichselian ice sheet on Svalbard inferred from high-resolution sea-floor morphology. Boreas 36, 286-306.

Ottesen, D., Dowdeswell, J.A., Rise, L., 2005. Submarine landforms and the reconstruction of fast-flowing ice streams within a large Quaternary ice sheet: The 2500-km-long Norwegian-Svalbard margin (57–80 N). Geological Society of America Bulletin 117, 1033-1050.

Overeem, I., Hudson, B.D., Syvitski, J.P.M., Mikkelsen, A.B., Hasholt, B., van den Broeke, M.R., Noël, B.P.Y., Morlighem, M., 2017. Substantial export of suspended sediment to the global oceans from glacial erosion in Greenland. Nature Geoscience 10, ngeo3046.

Palmer, S.J., Dowdeswell, J.A., Christoffersen, P., Young, D.A., Blankenship, D.D., Greenbaum, J.S., Benham, T., Bamber, J.L., Siegert, M.J., 2013. Greenland subglacial lakes detected by radar. Geophysical Research Letters 40, 6154-6159.

Parker, G., Fukushima, Y., Pantin, H.M., 1986. Self-accelerating turbidity currents. Journal of Fluid Mechanics 171, 145-181.

Pattyn, F., 2010. Antarctic subglacial conditions inferred from a hybrid ice sheet/ice stream model. Earth and Planetary Science Letters 295, 451-461.

Peakall, J., McCaffrey, W.D., Kneller, B.C., 2000. A Process Model for the Evolution, Morphology, and Architecture of Sinuous Submarine Channels. Journal of Sedimentary Research 70, 434-448.

Peakall, J., Sumner, E.J., 2015. Submarine channel flow processes and deposits: A process-product perspective. Geomorphology 244, 95-120.

Piper, D.J.W., Hiscott, R.N., Normark, W.R., 1999. Outcrop-scale acoustic facies analysis and latest Quaternary development of Hueneme and Dume submarine fans, offshore California. Sedimentology 46, 47-78.

Pirmez, C., Imran, J., 2003. Reconstruction of turbidity currents in Amazon Channel. Marine and Petroleum Geology 20, 823-849.

Pope, E.L., Talling, P.J., Carter, L., Clare, M.A., Hunt, J.E., 2017. Damaging sediment density flows triggered by tropical cyclones. Earth and Planetary Science Letters 458, 161-169.

Pope, E.L., Talling, P.J., Ó Cofaigh, C., 2018. The relationship between ice sheets and submarine mass movements in the Nordic Seas during the Quaternary. Earth-Science Reviews 178, 208-256.

Powell, R.D., 1990. Glacimarine processes at grounding-line fans and their growth to ice-contact deltas. Geological Society, London, Special Publications 53, 53-73.

Powell, R.D., 1991. Grounding-line systems as second-order controls on fluctuations of tidewater termini of temperate glaciers. Geological Society of America Special Papers 261, 75-94.

Powell, R.D., 2003. Subaquatic landsystems: fjords. Glacial Landsystems, 313-347.

Powell, R.D., Alley, R.B., 1997. Grounding-Line Systems: Processes, Glaciological Inferences and the Stratigraphic Record. Geology and seismic stratigraphy of the Antarctic Margin, 2, 169-187.

Powell, R.D., Domack, E., 1995. Modern glaciomarine environments. Glacial environments 1, 445-486.

Powell, R.D., Molnia, B.F., 1989. Glacimarine sedimentary processes, facies and morphology of the south-southeast Alaska shelf and fjords. Marine Geology 85, 359-390.

Prior, D.B., Bornhold, B.D., Wiseman, W.J., Lowe, D.R., 1987. Turbidity current activity in a British Columbia fjord. Science 237, 1330-1333.

Robinson, P., Dowdeswell, J.A., 2011. Submarine landforms and the behavior of a surging ice cap since the last glacial maximum: The open-marine setting of eastern Austfonna, Svalbard. Marine Geology 286, 82-94.

Rui, L., Rebesco, M., Casamor, J.L., Laberg, J.S., Rydningen, T.A., Caburlotto, A., Forwick, M., Urgeles, R., Accettella, D., Lucchi, R.G., Delbono, I., Barsanti, M., Demarte, M., Ivaldi, R., 2019. Geomorphology and development of a high-latitude channel system: the INBIS channel case (NW Barents Sea, Arctic). arktos.

Schoof, C.G., Hewitt, I.J., Werder, M.A., 2012. Flotation and free surface flow in a model for subglacial drainage. Part 1. Distributed drainage. Journal of Fluid Mechanics 702, 126-156.

Schumann, K., Völker, D., Weinrebe, W.R., 2012. Acoustic mapping of the Ilulissat Ice Fjord mouth, West Greenland. Quaternary Science Reviews 40, 78-88.

Schumm, S.A., Lichty, R.W., 1965. Time, space, and causality in geomorphology. American Journal of Science 263, 110-119.

Schwenk, T., Spieß, V., Breitzke, M., Hübscher, C., 2005. The architecture and evolution of the Middle Bengal Fan in vicinity of the active channel–levee system imaged by high-resolution seismic data. Marine and Petroleum Geology 22, 637-656.

Shreve, R.L., 1972. Movement of water in glaciers. Journal of Glaciology 11, 205-214.

Solheim, A., Faleide, J.I., Andersen, E.S., Elverhøi, A., Forsberg, C.F., Vanneste, K., Uenzelmann-Neben, G., Channell, J.E.T., 1998. Late Cenozoic seismic stratigraphy and glacial geological development of the East Greenland and Svalbard–Barents Sea continental margins. Quaternary Science Reviews 17, 155-184.

Stokes, C.R., 2018. Geomorphology under ice streams: Moving from form to process. Earth Surface Processes and Landforms 43, 85-123.

Streuff, K., Ó Cofaigh, C., Noormets, R., Lloyd, J.M., 2017. Submarine landforms and glacimarine sedimentary processes in Lomfjorden, East Spitsbergen. Marine Geology 390, 51-71.

Streuff, K., Ó Cofaigh, C., Noormets, R., Lloyd, J.M., 2018. Submarine landform assemblages and sedimentary processes in front of Spitsbergen tidewater glaciers. Marine Geology 402, 209-227.

Surpless, K.D., Ward, R.B., Graham, S.A., 2009. Evolution and stratigraphic architecture of marine slope gully complexes: Monterey Formation (Miocene), Gaviota Beach, California. Marine and Petroleum Geology 26, 269-288.

Symons, W.O., Sumner, E.J., Talling, P.J., Cartigny, M.J.B., Clare, M.A., 2016. Large-scale sediment waves and scours on the modern seafloor and their implications for the prevalence of supercritical flows. Marine Geology 371, 130-148.

Syvitski, J.P.M., 1989. On the deposition of sediment within glacier-influenced fjords: oceanographic controls. Marine Geology 85, 301-329.

Syvitski, J.P.M., Andrews, J.T., Dowdeswell, J.A., 1996. Sediment deposition in an iceberg-dominated glacimarine environment, East Greenland: basin fill implications. Global and Planetary Change 12, 251-270.

Syvitski, J.P.M., Farrow, G.E., 1989. Fjord sedimentation as an analogue for small hydrocarbon-bearing fan deltas. Geological Society, London, Special Publications 41, 21-43.

Syvitski, J.P.M., Shaw, J., 1995. Sedimentology and geomorphology of fjords, in: Perillo, G.M.E. (Ed.), Developments in sedimentology. Elsevier, Amsterdam, pp. 113-178.

Talling, P.J., Paull, C.K., Piper, D.J.W., 2013. How are subaqueous sediment density flows triggered, what is their internal structure and how does it evolve? Direct observations from monitoring of active flows. Earth-Science Reviews 125, 244-287.

Tasianas, A., Martens, I., Bünz, S., Mienert, J., 2016. Mechanisms initiating fluid migration at Snøhvit and Albatross fields, Barents Sea. arktos 2, 26.

Tedesco, M., Willis, I.C., Hoffman, M.J., Banwell, A.F., Alexander, P., Arnold, N.S., 2013. Ice dynamic response to two modes of surface lake drainage on the Greenland ice sheet. Environmental Research Letters 8, 034007.

Vorren, T.O., Laberg, J.S., 1997. Trough mouth fans—palaeoclimate and ice-sheet monitors. Quaternary Science Reviews 16, 865-881.

Walder, J.S., Fowler, A., 1994. Channelized subglacial drainage over a deformable bed. Journal of Glaciology 40, 3-15.

Wiles, G.C., Calkin, P.E., Post, A., 1995. Glacier fluctuations in the Kenai Fjords, Alaska, USA: an evaluation of controls on iceberg-calving glaciers. Arctic and Alpine Research 27, 234-245.

Willis, I.C., Pope, E.L., Leysinger Vieli, G.J.M.C., Arnold, N.S., Long, S., 2016. Drainage networks, lakes and water fluxes beneath the Antarctic ice sheet. Annals of Glaciology 57, 96-108.

Wynn, R.B., Cronin, B.T., Peakall, J., 2007. Sinuous deep-water channels: Genesis, geometry and architecture. Marine and Petroleum Geology 24, 341-387.

Wynn, R.B., Stow, D.A.V., 2002. Classification and characterisation of deep-water sediment waves. Marine Geology 192, 7-22.

Zwally, H.J., Abdalati, W., Herring, T., Larson, K., Saba, J.L., Steffen, K., 2002. Surface melt-induced acceleration of Greenland ice-sheet flow. Science 297, 218-222.

Figures

Fig. 1a) – c). Location maps of glaciers and fjords in northwest Greenland. Background bathymetry is greyscale IBCAO with 200 m contours (Jakobsson et al., 2012). Average ice velocities for the Greenland Ice Sheet between 2016 and 2017 is from MEaSUREs Ice Sheet Velocity Mosaics V2 (Joughin et al., 2015, updated 2017). Glacier names are taken from Bjørk et al. (2015). IS = Issuusarsuit Sermiat. Diet = Dietrichson. SA = Sermeq Avanarleq. SK = Sermeq Kujalleq. QS = Qeqertarsuup Sermia. KS = Kakiffaat Sermiat. NS = Nunatakassaap Sermia. AkS = Kaullilassaap Sermia. UI = Upernavik Isstrøm. UmI = Umiammakku Sermiat. Sis = Sisoortartukassak. SerA = Sermeq Avannarleq. AlS = Alianaatsup Sermia. Kangil = Kangilernata Sermia.

Fig. 2a) – c). Location maps of glaciers and fjords in southeast Greenland. Background bathymetry is greyscale IBCAO with 200 m contours (Jakobsson et al., 2012). Average ice velocities for the Greenland Ice Sheet between 2016 and 2017 is from MEaSUREs Ice Sheet Velocity Mosaics V2 (Joughin et al., 2015, updated 2017). Glacier names are taken from Bjørk et al. (2015). UK = Uummannap Kangertiva. K = Katterooq. KBS = Kangertittivaq Bernstorff Isfjord. UmK = Umiiviip Kangertiva. PK = Pukukkat Kangertivat. QK = Qeertartivatsaap Kangertiva. APB = A.P. Bernstorff Glacier. Fim = Fimbulglacier. KJV = K.J.V. Streenstrup Nordre Bræ.

Fig. 3. a) BedMachine v3 bedrock topography (m) (Morlighem et al., 2017). b) Subglacial hydrologic potential (Pa) of the Greenland Ice Sheet derived from 150 m surface and bed elevation grids contained in the BedMachine v3 datasets. c) Drainage catchments basins for Greenland.

Fig. 4a) – d). Examples of monthly runoff output for the Greenland Ice Sheet calculated using RACMO2.3 for four different months in 2017. a) February, 2017. b) May, 2017. c) August, 2017. d) November, 2017.

Fig. 5. a) to c) Examples of Type 1 submarine channels and associated fjord characteristics. All examples shown are from northwest Greenland GZW = Grounding-Zone Wedge. a) Submarine channel in Noorujupaluk, offshore the calving margin of Carlos Glacier to the north and Mohn Glacier. b) Submarine channel in Ryder Isfjord. c) Submarine channel in Ussing Isfjord offshore of Sermeq Kujalleq Glacier. All channels originate at moraines or grounding-zone wedges and are characterised by terraces. Fjords have relatively smooth bottoms. Background is Landsat satellite imagery from August 2016.

Fig. 6. a) to d) Examples of Type 2 submarine channels. With the exception of a) all the examples shown are from southeast Greenland. a) Submarine channel offshore of Illullip Sermia. b) Submarine channel offshore of Guldfaxe Glacier in Uummannap Kangertiva. c) Submarine channels in Tasiialak Fjord. d) Submarine channel in Nørrearm Fjord. Channels originate from moraines associated with active glacier fronts (a and b) or moraines from which glaciers have retreated from (c and d). Type 2 channels are generally shorter than Type 1 channels and are not associated with terraces. Background is Landsat satellite imagery from September 2016

Fig. 7. Examples of characteristic fjords which do not contain channels. a) Illaarsuaauq Fjord. MoGl = Morrel Glacier. DSGl = Döcker Smith Glacier. b) Qeetartivatsaap Kangertiva. KaGl = Kattilertarpia Glacier. BrGl = Brückner Glacier. HiGl = Heim Glacier. Fjords contain elongate ridges, minibasins, overdeepening, reverse slopes, bedrock outcrops or do not contain large moraines and grounding-

zone wedges. Background is Landsat 8 satellite imagery from August and September 2016.Fig. 8. Box and whisker plots of characteristics, which could control channel presence/absence. NW CP = Northwest Greenland Channel Present; NW CA = Northwest Greenland Channel Absent; SE CP = Southeast Greenland Channel Present; SE CA = Southeast Channel Absent; All CP = All Channel Present; All CA = All Channel Absent.

Fig. 9. Box and whisker plots of channel, fjord and catchment characteristics for systems which contain channels. NW = Northwest Greenland; SE = Southeast Greenland; T1 = type 1 channels; T2 = type 2 channels.

Fig. 10. Schematic of the general criteria thought to control/characterise glacier-fed catchments, which do and do not contain submarine channels. a) Channels are more likely to be associated with: glacier catchment with areas >100 km^2, a stable ice front, high meltwater sedimentation regimes, and fjords that are characterised by consistent slope gradients and contain sufficient sedimentary substrate to allow channel incision to occur. b – c) Channels are more likely to be absent where: glacier catchments are small (<100 km^2), sedimentation rates are low, the ice front is unstable, the fjord floor is characterised by thin or absent sedimentary substrate, and highly variable seafloor gradients, including those with reverse slopes or overdeepenings.

Fig. 11. Examples of submarine channels identified offshore of marine-terminating glaciers in Alaska. As observed offshore Greenland, submarine channels are the dominant feature of the fjords and occur where the seafloor is relatively smooth with a consistent seaward sloping gradient. Inset figure shows the location of a – c). a) Submarine channel offshore of John Hopkins Glacier. JHG = John Hopkins Glacier. JHI = John Hopkins Inlet. b) Submarine channel in Tarr Inlet. MarGl = Margerie Glacier. c)

Submarine channel in Endicott Arm associated with a moraine from a previous advance of Dawes Glacier. Background is Landsat 8 satellite imagery acquired in September 2018.

Tables

Table 1. Characteristics of identified submarine channels and glacier catchments which terminate in each fjord associated with a submarine channel. X* refers to fjords where no moraine or grounding-zone wedge is identified but the channel head is not covered by the bathymetry. N/A refers to fjords which are completely filled by gullies which feed a central submarine channel preventing an independent fjord gradient from being calculated. No average runoff or glacier catchment area are provided for Ikerasak Ataa Sund as the channel is fed by Equip Sermia and a large proglacial river which is fed by three other glacier which do not terminate in the fjord.

Table 2. Characteristics of glacier catchments which terminate in fjords which are not associated with submarine channels. ✓* = Small retreat moraines are present.

Table 3. t-test results comparing the difference between fjord and catchment characteristics of systems which do and do not contain channel systems. Systems which do and do not contain channels are compared only in northwest Greenland, in southeast Greenland and in both regions.

Table 4. t-test results of the statistical difference between individual morphological and catchment characteristics of type 1 and type 2 channel systems.

Table 5. Characteristics of fjords/outlets around Alaska and South Georgia. Ticks identify where a morphological feature is present. Crosses identify where a morphological feature is absent. L =

Lineations, CSB = Crescentic Submarine Bedforms. Additional references (Brown et al., 1982; Wiles et al., 1995; Gordon et al., 2008; Goff et al., 2012; Hodgson et al., 2014).

Table 6. Characteristics of fjords/outlets around Svalbard. Ticks identify where a morphological feature is present. Crosses identify where a morphological feature is absent. E = Eskers, T = Transverse Ridges, L = Lineations, C = Crevasse-filled ridges, CT = Crag and Tails, SC = Subglacial Channel, P = Pockmarks, MTD = Mass Transport Deposit, D = Drumlin. References (Ottesen and Dowdeswell, 2006, 2009; Ottesen et al., 2008, 2017; Baeten et al., 2010; Forwick et al., 2010, 2016; Robinson and Dowdeswell, 2011; Kempf et al., 2013; Hansen, 2014; Burton et al., 2016a, b; Farnsworth et al., 2017; Flink et al., 2017, 2018; Streuff et al., 2017, 2018; Leister, 2018).

Table 1

Fjord	Glacier	Moraine/GZW	Glacier Catchment Area (km²)	Ice Flux (km³a⁻¹)	Average Runoff (km³a⁻¹)	Peak Runoff (km³a⁻¹)	Total Runoff (km³a⁻¹)	Average Fjord Gradient (°)	Average Channel Slope (°)	Channel Length (km)	Channel Sinuosity	Average Channel Width (m)	Average Channel Depth (m)	Channel Type
Northwest Greenland														
Torsukattak	Sermeq Avannarleq Alianaatsup Sermia	✓	44000	6.95	0.307	1.9	3.687	2.28	1.98	>16	1.373	446	21.2	Type 1
Noorujupaluk	Carlos Cornell	✓	950	0.77	0.019	0.129	0.229	1.67	1.88	24.48	1.077	294	10.5	Type 1
Ryder Isfjord	Ikissuup Sermersua	✓	425	1.29	0.066	0.392	0.788	2.71	2.09	22.48	1.097	199	16	Type 1
	Illullip Sermia	✓	39700	4.96	0.205	1.441	2.464	1.68	2.21	5.58	1.129	170	13.4	Type 2
Itilliarsuup Kangerlua	Kangilleq	✓	115	0.73	0.023	0.129	0.278	N/A	3.5	22.9	1.425	207	34.2	Type 1
Ussing Isfjord	Sermeq Kujalleq	✓	2900	3.86	0.195	1.359	2.345	N/A	2.11	37.66	1.194	288	40.2	Type 1
Upernavik Isfjord	Upernavik Isstrøm	✓	4200	2.22	0.118	0.8	1.413	1.77	2.61	5.2	1.092	108	12.7	Type 2
	Akullikassaap Sermia	✓	115	3.87 x 10^{-3}	0.016	0.102	0.19	2.64	1.76	3.68	1.103	118	21.9	Type 2
	Kjer	✓	28000	1.08	0.163	1.21	1.954	N/A	2.8	>11.45	1.15	375	46.3	Type 1
Ikerasak Ataa Sund	Equip Sermia	✓		3.86				1.74	2.45	>5.03	1.12	321	28.9	Type 2
Kangilleq	Rink Isbrae	✓	48700	12.49	0.139	0.869	1.664	3.17	3.2	9.3	1.479	154	23.1	Type 2

Average			16900	3.44	0.125	0.833	1.501	2.21	2.42	>14.89	1.204	244	24.4	
Southeast Greenland														
Torsukattak	Frederiksborg	✓	70	0.2	0.01	0.047	0.125	N/A	2.8	13.94	1.127	111	13.1	Type 2
		✓	420	1.13 x 10^{-3}	0.043	0.088	0.513	1.3	1.57	3.79	1.111	165	10.9	Type 2
		✓	900	3.23 x 10^{-3}	0.031	0.17	0.377	1.68	2.75	5.23	1.054	110	10.3	Type 2
Tasiilak		✓	180	1.13 x 10^{-3}	0.014	0.076	0.164	1.58	1.95	4.89	1.079	100	5	Type 2
Pukukkat Kangertivat		✓	875	8.97 x 10^{-2}	0.047	0.258	0.562	0.91	2.11	2.3	1.035	79	7.8	Type 2
Ikertivaq		✓	4500	1.77	0.049	0.264	0.583	2.46	3.7	>3.97	1.034	76	18.2	Type 2
Ikertivaq		✓	170	2.06	0.015	0.073	0.184	5.34	4.31	12.04	1.064	105	18.3	Type 2
Ikeq Kogebugt		x*	16500	5.68	0.068	0.301	0.821	3.12	1.85	>9.51	1.106	246	23.3	Type 1
Ikeq Kogebugt		✓	10900	11.79	0.058	0.275	0.694	3.31	3.54	6.31	1.048	173	29.5	Type 2
		✓	370	1.18	0.034	0.168	0.405	2.54	2.99	8.25	1.074	140	12.1	Type 2
Napasorsuup Kangerlua		✓	850	1.33	0.035	0.176	0.424	1.14	2.31	2.97	1.036	120	7.5	Type 2
Paatusoq		✓	140	3.38 x 10^{-3}	0.029	0.123	0.344	0.98	2.13	10.27	1.259	108	9.6	Type 2
Lindenow		✓	175	3.87 x 10^{-4}	0.042	0.177	0.505	3.46	2.68	11.75	1.181	170	33.7	Type 2
Avaaqqat Kangerluat		x*	10000	5.5	0.058	0.256	0.695	2.13	8.16	>2.81	1.186	84	20.7	Type 2

Sikuijivitteq		✓	4700	3.3	0.124	0.572	1.494	2.09	2.08	14.01	1.25	110	13.8	Type 2
Anoritup Kangerlua		✓	685	2.53 x 10^{-3}	0.035	0.173	0.422	3.35	2.89	6.08	1.077	154	35.1	Type 1
Danell		✓	890	0.44	0.092	0.362	1.107	1.26	2.71	2.16	1.022	85	5.8	Type 2
Norrearm		✓	500	>0.15	0.039	0.161	0.47	1.89	2.94	6.39	1.406	115	19.1	Type 2
Lindenow		✓	480	0.44	0.043	0.189	0.518	1.43	1.65	4.93	1.163	120	7.8	Type 2
	Heimdal	✓	3800	0.89	0.129	0.598	1.549	3.46	2.71	3.17	1.055	63	5.1	Type 2
	Garm Skirner Bjerge	x*	3750	1.4 x 10^{-3}	0.068	0.303	0.813	2.85	1.65	>16.69	1.227	184	37.7	Type 1
Uummannap Kangertiva	Guldfaxe	✓	1800	1.65	0.079	0.356	0.944	2.41	3.3	17.37	1.656	128	12.7	Type 2
Kattertooq	Apusiikajik	✓	3800	1.28	0.105	0.346	1.258	3.64	1.64	33.99	1.143	148	19	Type 1
Kangertittivaq Bernstoff Isfjord	A. P. Bernstorf Gletscher	x*	4400	6.47	0.12	0.568	1.441	2.91	2.33	>4.96	1.304	178	12.6	Type 2
Kangertittivaq Bernstoff Isfjord	Sleipner	x*	4350	3.38 x 10^{-3}	0.066	0.301	0.787	2.91	2.41	>5.7	1.115	302	34.1	Type 1
Kangerlussuaq	Kangerlussuaq	x*	55000	23.63	0.334	1.964	4.008	1.15	1.8	>8.45	1.158	196	5.1	Type 2
Average			5008	2.71	0.068	0.325	0.815	2.37	2.73	>8.22	1.157	137	16.5	

Table 2

Fjord	Glacier	Moraine/ GZW	Glacier Catchment Area (km^2)	Ice Flux (km^3a^{-1})	Average Runoff (km^3a^{-1})	Peak Monthly Runoff (km^3a^{-1})	Total Runoff (km^3a^{-1})	Average Fjord Gradient (°)
Northwest Greenland								
Pulsilik/De Dødes		✓*	120	0.067	0.009	0.064	0.107	5.72
Pulsilik/De Dødes		✓*	390	0.386	0.025	0.191	0.305	6.18
Pulsilik/De Dødes		✓*	280	0.174	0.018	0.135	0.218	5.87
Pulsilik/De Dødes		✓*	250	0.138	0.2	0.139	0.238	6.68
Illaarsuaauaq		x	70	0.002	0.009	0.058	0.106	5.26
Illut		✓*	430	0.232	0.069	0.15	0.229	3.96
Meteorbugt	Yngvar Nielsen	x	1070	0.875	0.04	0.287	0.478	5.31
Noorujupaluk	Gades	✓	3105	2.153	0.041	0.303	0.493	5.28
	Morrell	✓	130	0.268	0.014	0.102	0.166	4.54
		x	510	1.485	0.039	0.28	0.472	3.61
	Döcker Smith	x	4100	1.546	0.031	0.226	0.375	2.73
	Rink	x	4300	3.09	0.026	0.195	0.315	4.11
	Issuusarsuit Sermiat	x	3740	1.512	0.04	0.276	0.485	
	Nansen	x	580	1.18	0.051	0.065	0.109	3.81
Duneira Bugt	Sverdrup	x	1540	5.996	0.086	0.597	1.036	
Duneira Bugt	Dietrichson	✓	300	2.511	0.037	0.254	0.439	4.63
	Hayes	x	130	6.851	0.021	0.128	0.256	1.8
Kullorsuup Kangerlua		x	120	4.64	0.02	0.124	0.237	1.72
Kullorsuup Kangerlua		x	380	1.1	0.052	0.345	0.624	4.11
Kullorsuup Kangerlua		x	130	3.916	0.017	0.103	0.2	4.14
Kullorsuup Kangerlua	Nunatakassap Sermia	x	720	8.972	0.077	0.529	0.926	1.51
Kangerlussuaq	Qetqertarsuup Sermia	x						
Giesecke	Kakiffaat Sermiat		910	0.645	0.084	0.579	1.002	1.1
Isfjord		x	31500	5.649	0.148	1.031	1.772	12.2
	Umiammakku Isbrae	✓	130	3.916				4.14
Average			2290	2.388	0.05	0.268	0.46	4.47

Southeast Greenland								
Kangerluluk		✓	790	1.104	0.057	0.259	0.688	0.93
Avaaqqat Kangerluat		✓	3900	0.746	0.114	0.502	1.371	1.24
Anorituup Kangerlua		x	1100	3.223	0.117	0.544	1.401	1.22
Napasorsuup Kangerlua		✓	5300	6.75	0.09	0.424	1.077	0.81
		x	14100	5.953	0.136	0.742	1.632	0.97
Timmiarmiit Kangertivat		x	5600	1.727	0.064	0.344	0.769	4.82
Umiiviip Kangertiva		x	30	7.634×10^{-5}	0.003	0.013	0.035	1.6
Nattivit Kangertivat	Bussemandgletsjer	✓	270	6.57×10^{-5}	0.0352	0.181	0.422	0.93
	Apuseeq	x	110	5.63×10^{-4}	0.02	0.085	0.237	8.76
	K. J. V. Steenstrup Nordre Brae	x	3820	2.396	0.146	0.784	1.75	1.95
Qeertartivatsaap Kangertiva	Heim	✓	900	0.036	0.046	0.233	0.555	2.88
	Polaric	x	3200	1.361	0.136	0.742	1.632	0.81
Nansen	Christian IV	x	12500	2.994	0.444	2.615	5.326	1.22
Average			3970	2.022	0.108	0.574	1.3	2.16

Table 3

Characteristic	Region	p-value
Catchment area	Northwest	0.056
	Southeast	0.68
	All	0.048
Ice flux	Northwest	0.387
	Southeast	0.62
	All	0.485
Average runoff	Northwest	0.043
	Southeast	0.243
	All	0.516
Peak monthly runoff	Northwest	0.021
	Southeast	0.225
	All	0.441
Total runoff	Northwest	0.021
	Southeast	0.243
	All	0.273
Fjord slope gradient	Northwest	0
	Southeast	0.761
	All	0.007

Table 4

Characteristic	p-value
Channel width	0.001
Channel length	0.004
Channel depth	0.002
Channel sinuosity	0.766
Channel gradient	0.086
Fjord gradient	0.046
Catchment area	0.708
Average monthly runoff	0.376
Peak monthly runoff	0.376
Total runoff	0.415
Ice flux	0.281

Table 5

Fjord	Glacier	Channel Present	Catchment area (km^2)	Ice Flux ($km^3 a^{-1}$)	Moraine / Grounding zone wedge	Sediment cover	Exposed bedrock	Consistent Downslope Gradient	Other features
Alaska									
Endicott Arm	Dawes Glacier	✓	604	0.6	✓	✓	x	✓	CSB
John Hopkins Inlet	John Hopkins Glacier	✓	254	0.6	✓	✓	x	✓	
John Hopkins Inlet	Lamplugh Glacier	x	161	0.16	✓	✓	x	✓	CSB
Tarr Inlet	Grand Pacific Glacier Margerie Glacier	✓	565 182	0.1 0.1	✓	✓	x	✓	
Rendu Inlet	Rendu Glacier	✓	128		✓	✓	x	✓	CSB
Disenchantment Bay	Hubbard Glacier	x	3900		x	✓	✓	x	
Aialik Bay	Aialik Glacier	x	70		✓	✓	✓	x	L
Holgate Arm	Holgate Glacier	x	69		✓	✓	x	x	
Northwestern Fjord	Northwestern Glacier	x	72		✓	✓	✓	✓	CSB
South Georgia									
Royal Bay	Ross Glacier Hindle Glacier	x	100.7		✓	✓	x	✓	SC
Cumberland Bay East	Nordenskjold Glacier	x	135.5		✓	✓	x	✓	
Cumberland Bay West	Neumayer Glacier	x	86.4		✓	✓	x	✓	MTD
Stormness bay		x			✓	✓	x	x	
Husvik Bay									
Antarctic bay	Crean Glacier	x	62		✓	✓	✓	x	L, E
Possession Bay		x			✓	✓	x	x	
King Haakon Bay	Briggs Glacier	x			✓	✓	✓	x	
Drygalski Fjord	Jenkins Glacier Risting Glacier	x			✓	✓	x	✓	

Table 6

Fjord	Glacier	Channel Present	Catchment area (km^2)	Ice Flux ($km^3 a^{-1}$)	Moraine / Grounding zone wedge	Sediment cover	Exposed bedrock	Consistent Downslope Gradient	Other features
Keulenfjorden	Doktorbreen	x	95	0.0002	✓	✓	x	x	E, T, MTD, P
Keulenfjorden	Liestølbreen	x	99	0.0047	✓	✓	x	x	E, T, MTD, P
Keulenfjorden	Nathorstbreen	x	318.8	0.0436	✓	✓	x	x	E, T, MTD, P
Rindersbukta	Paulabreen	x	56.4	0.001	✓	x	x	x	E, L, C, MTD
Rindersbukta	Bakaninbreen	x	60.8		✓	x	x	x	E, L, C, MTD
Rindersbukta	Scheelebreen	x	58.4		✓	x	x	x	E, L, C, MTD
Templefjorden	Tunabreen	x	137.6	0.244	✓	✓	x	✓	L, MTD
Templefjorden	Von Postbreen	x	174		✓	✓	x	✓	L, MTD
Billefjorden	Nordenskiöldbreen	x	169.5	0.0816	✓	x	✓	x	L, P, MTD
Borebukta	Borebreen	x	87	0.0051	✓	x	x	x	L, C, MTD
Borebukta	Nansenbreen	x	31.1	0.0028	✓	x	x	x	L, C, MTD
Yoldiabukta	Wahlenbergbreen	x	104.2	0.0113	✓	x	x	x	L, C, MTD
Trygghamna	Harrietbreen Kjerulfbreen	x			✓	✓	x	✓	L, MTD, P
Ymerbukta	Esmarkbreen	x	33.4	0.0036	✓	✓	x	✓	MTD, P
St Jonsfjorden	Osbornebreen	x	130.6	0.0478	✓	x	x	✓	L, C, MTD
St Jonsfjorden	Konowbreen	x	39.9	0.0108	✓	x	x	✓	L, C, MTD
Kongsfjorden	Kongsbreen	x	153.9	0.25	✓	x	✓	x	L, CT, SC
Kongsfjorden	Kronebreen	x	509.8	0.3103	✓	x	✓	x	L, CT, SC
Kongfjorden	Blomstrandbreen	x	65.7	0.0137	✓	✓	x	x	L, MTD
Lilliehöökfjorden	Lilliehöökbreen	x	211.8	0.106	✓	✓	x	✓	L, D
Möllerfjorden	Kollerbreen	x	20.5	0.0121	✓	✓	✓	✓	L, MTD

Möllerfjorden	Mayerbreen	x	34.6	0.0189	✓	✓	✓	✓	L
Magdalenefjorden	Waggonwaybreen	x	29.1	0.0222	✓	x	✓	x	
Smeerenburgfjorden	Smeerrenburgbreen	x	95	0.0258	✓	✓	✓	✓	MTD
Liefdefjorden	Monacobreen	x	344.5	0.0907	✓	x	✓	x	L, MTD
Bockfjorden	Karlsbreen Friedrickbreen Børrebreen	x	151.5		✓	x	✓	✓	L, MTD
Woodfjorden	Vonbreen Abrahamsenbreen Elnabreen Johanbreen	x	315		✓	x	✓	✓	L, CT, D, E, P, MTD
Lomfjorden	Veteranen	x	300		x	x	✓	✓	L, D, MTD
Wahlenbergfjorden	Etonbreen	x	664.2	0.0411	✓	x	✓	✓	L, C, E, SC, MTD, CT
Hartogbukta	Austfonna	x			✓	x	✓	x	L, SC, D
	Sonklarbreen	x	207.2	0.0171	✓	x	x	x	L, E, SC, MTD
	Hochstetterbreen	x	589.2	0.012	✓	x	x	x	L, MTD
	Negribreen	x	916.2	0.001	✓	x	x	x	L, D, E, SC, MTD
	Besselsbreen	x	128.6	0.0065	✓	x	x	x	L, E, SC, MTD
	Koristkabreen	x	50	0.0017	✓	x	✓	x	L, MTD
	Pedasjenkobreen	x	36.2	0.0024	✓	x	✓	x	L, E, SC
	Hannbreen	x	22.8	0.001	✓	x	✓	x	L
Mohnbukta	Heuglinbreen Hayesbreen Königsbergbreen	x	119.7	0.0277	✓	x	x	x	L, E, MTD
	Duckwitzbreen	x	72.6	0.0002	✓	x	x	x	L, E
Freemansundet	Freemanbreen	x	72.6	0.0021	✓	x	x	x	L

Highlights

- Most complete inventory of submarine channels offshore Greenland
- Submarine channels are more common offshore of southeast Greenland
- Controls on channel formation are defined and used to construct conceptual model
- Observations from other glacier-influenced settings show support for these criteria

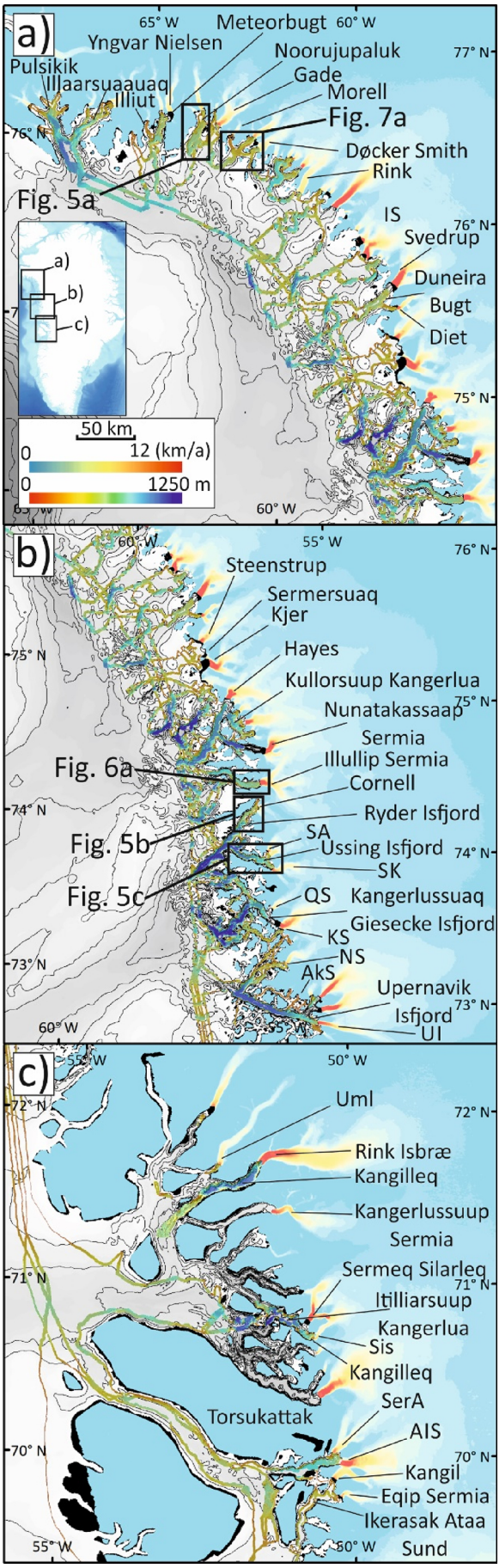
a)
Meteorbugt
Yngvar Nielsen
Noorujupaluk
Pulsikik
Gade
Illaarsuaaquaq
Morell
Illiut
Fig. 7a
Døcker Smith
Rink
Fig. 5a
IS
Svedrup
Duneira
Bugt
Diet
a)
b)
c)
50 km
0
12 (km/a)
0
1250 m
65° W
60° W
77° N
76° N
75° N
b)
Steenstrup
Sermersuaq
Kjer
Hayes
Kullorsuup Kangerlua
Nunatakassaap
Sermia
Fig. 6a
Illullip Sermia
Cornell
Ryder Isfjord
Fig. 5b
SA
Ussing Isfjord
SK
Fig. 5c
QS
Kangerlussuaq
Giesecke Isfjord
KS
NS
AkS
Upernavik
Isfjord
UI
60° W
55° W
76° N
75° N
74° N
73° N
c)
50° W
72° N
Uml
Rink Isbræ
Kangilleq
Kangerlussuup
Sermia
Sermeq Silarleq
Itilliarsuup
Kangerlua
Sis
Kangilleq
SerA
Torsukattak
AIS
Kangil
Eqip Sermia
Ikerasak Ataa
Sund
71° N
70° N
55° W

Figure 1

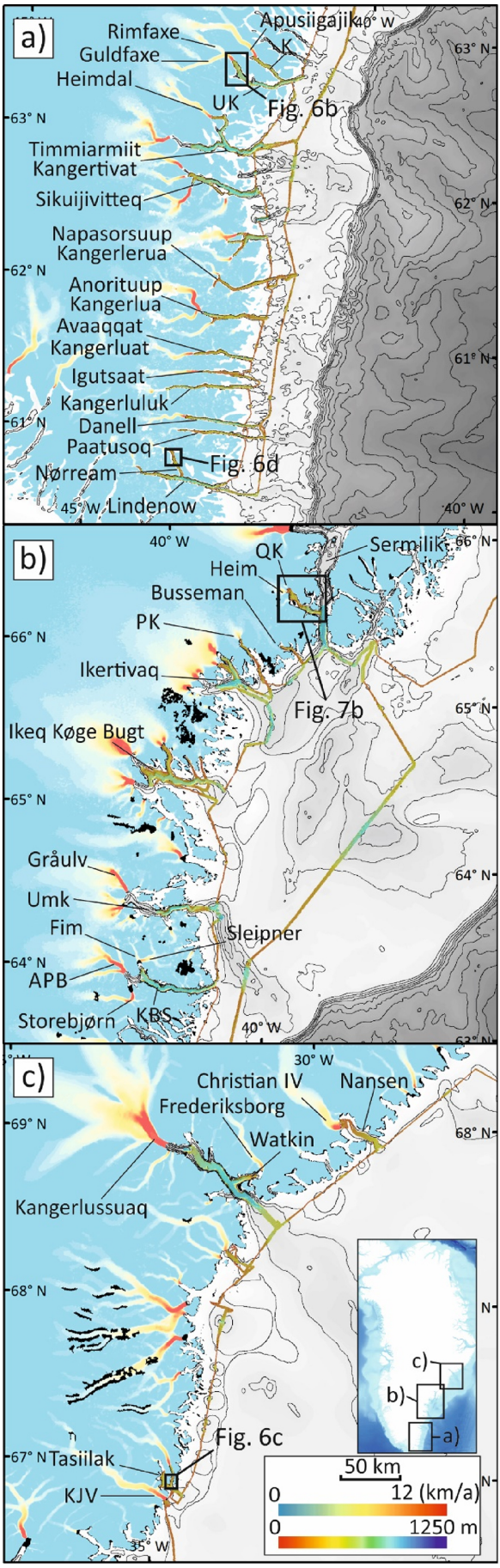
a)
Rimfaxe
Guldfaxe
Heimdal
Apusiigajik
K
UK
Fig. 6b
Timmiarmiit
Kangertivat
Sikuijivitteq
Napasorsuup
Kangerlerua
Anorituup
Kangerlua
Avaaqqat
Kangerluat
Igutsaat
Kangerluluk
Danell
Paatusoq
Fig. 6d
Nørream
Lindenow
63° N
62° N
61° N
40° W
45° W
b)
QK
Heim
Busseman
PK
Ikertivaq
Fig. 7b
Sermilik
Ikeq Køge Bugt
Gråulv
Umk
Fim
Sleipner
APB
Storebjørn
KBS
66° N
65° N
64° N
c)
Christian IV
Nansen
Frederiksborg
Watkin
Kangerlussuaq
69° N
68° N
67° N
30° W
35° W
Fig. 6c
Tasiilak
KJV
50 km
0
12 (km/a)
0
1250 m

Figure 2

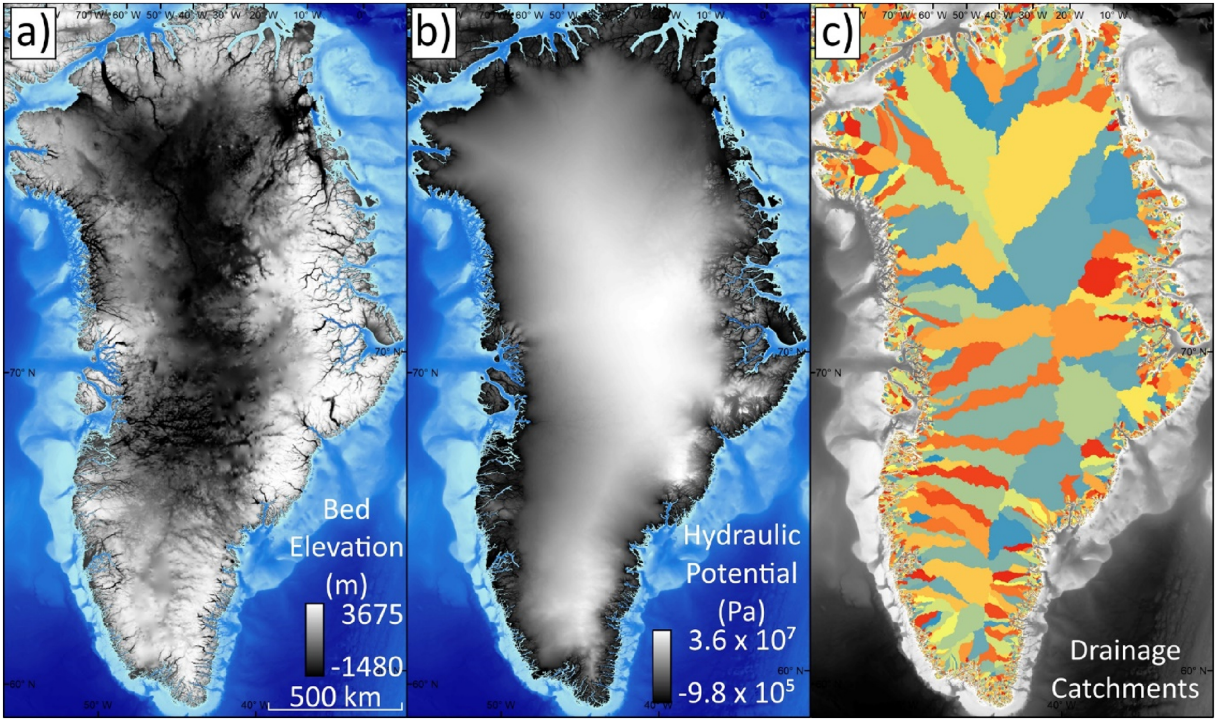
a)
Bed
Elevation
(m)
3675
-1480
500 km
b)
Hydraulic
Potential
(Pa)
3.6 x 10^7
-9.8 x 10^5
c)
Drainage
Catchments

Figure 3

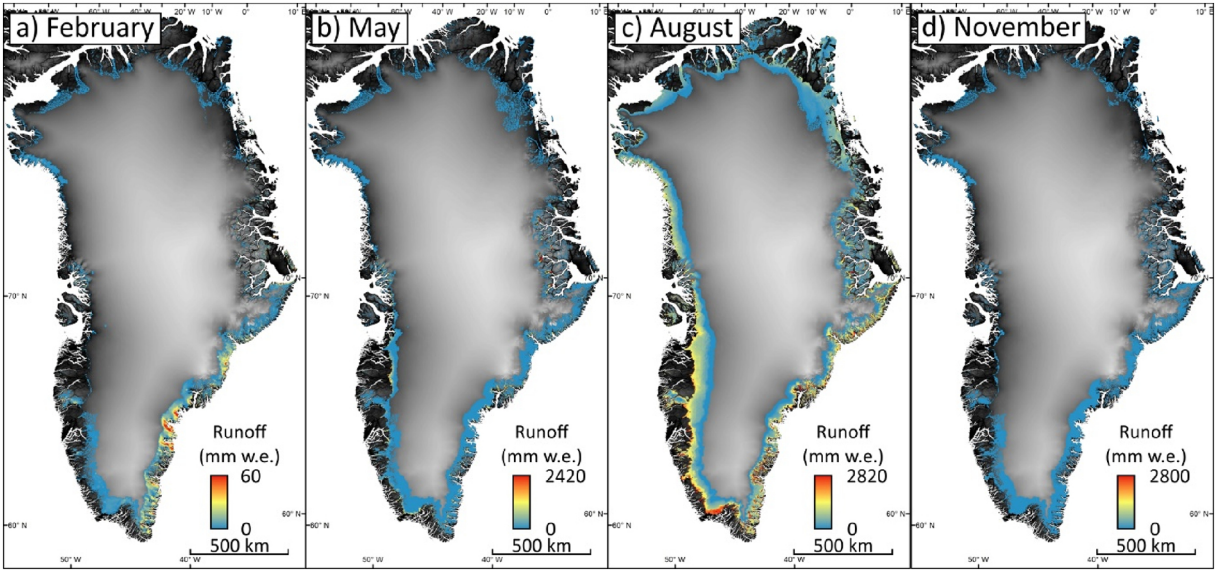
a) February
b) May
c) August
d) November
Runoff
(mm w.e.)
60
2420
2820
2800
0
500 km
70° N
60° N
50° W
40° W

Figure 4

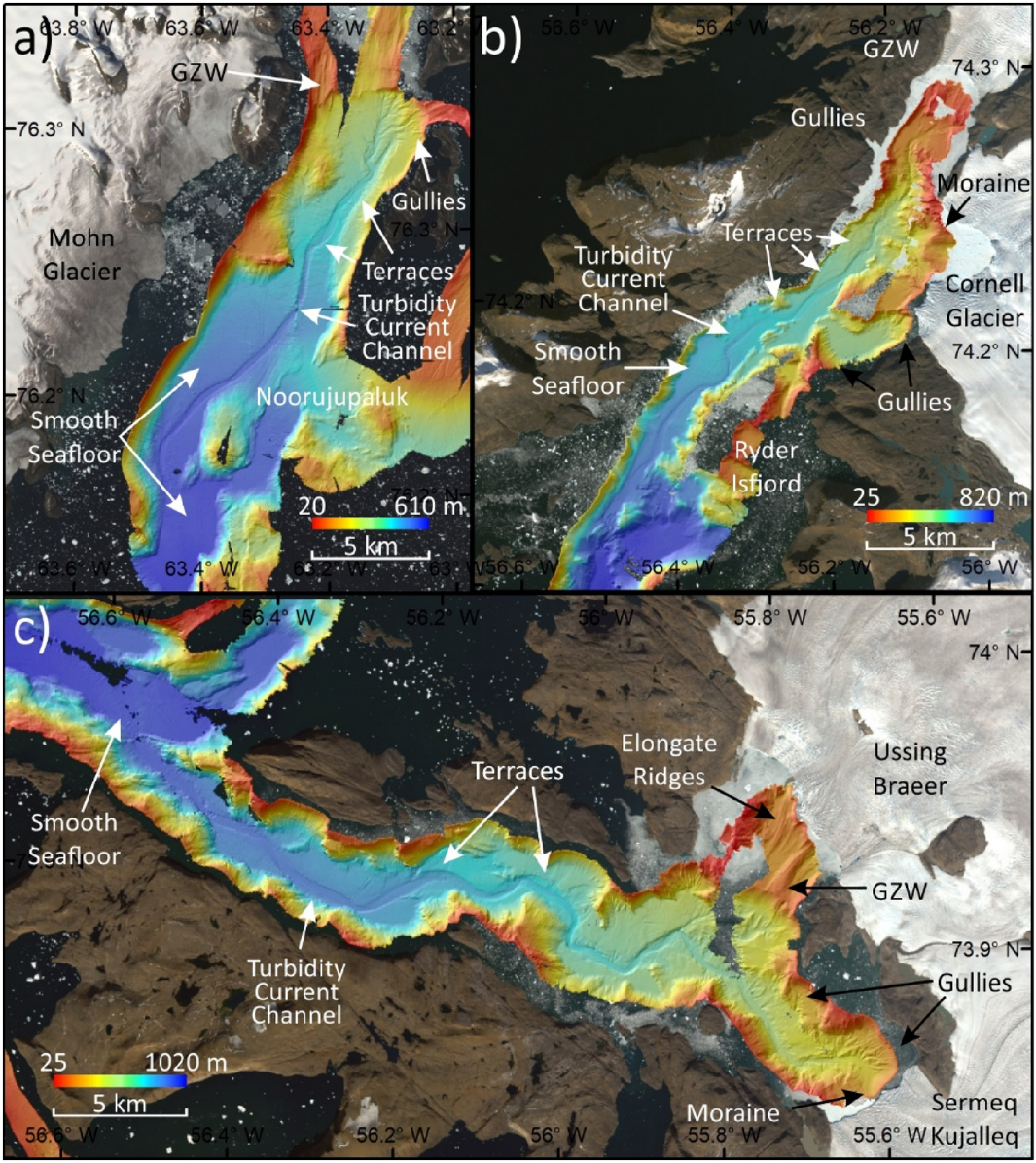
a)
GZW
Gullies
Mohn
Glacier
Terraces
Turbidity
Current
Channel
Noorujupaluk
Smooth
Seafloor
20
610 m
5 km
b)
GZW
Gullies
Moraine
Terraces
Turbidity
Current
Channel
Cornell
Glacier
Smooth
Seafloor
Gullies
Ryder
Isfjord
25
820 m
5 km
c)
Smooth
Seafloor
Terraces
Elongate
Ridges
Ussing
Braeer
GZW
Turbidity
Current
Channel
Gullies
25
1020 m
5 km
Moraine
Sermeq
Kujalleq

Figure 5

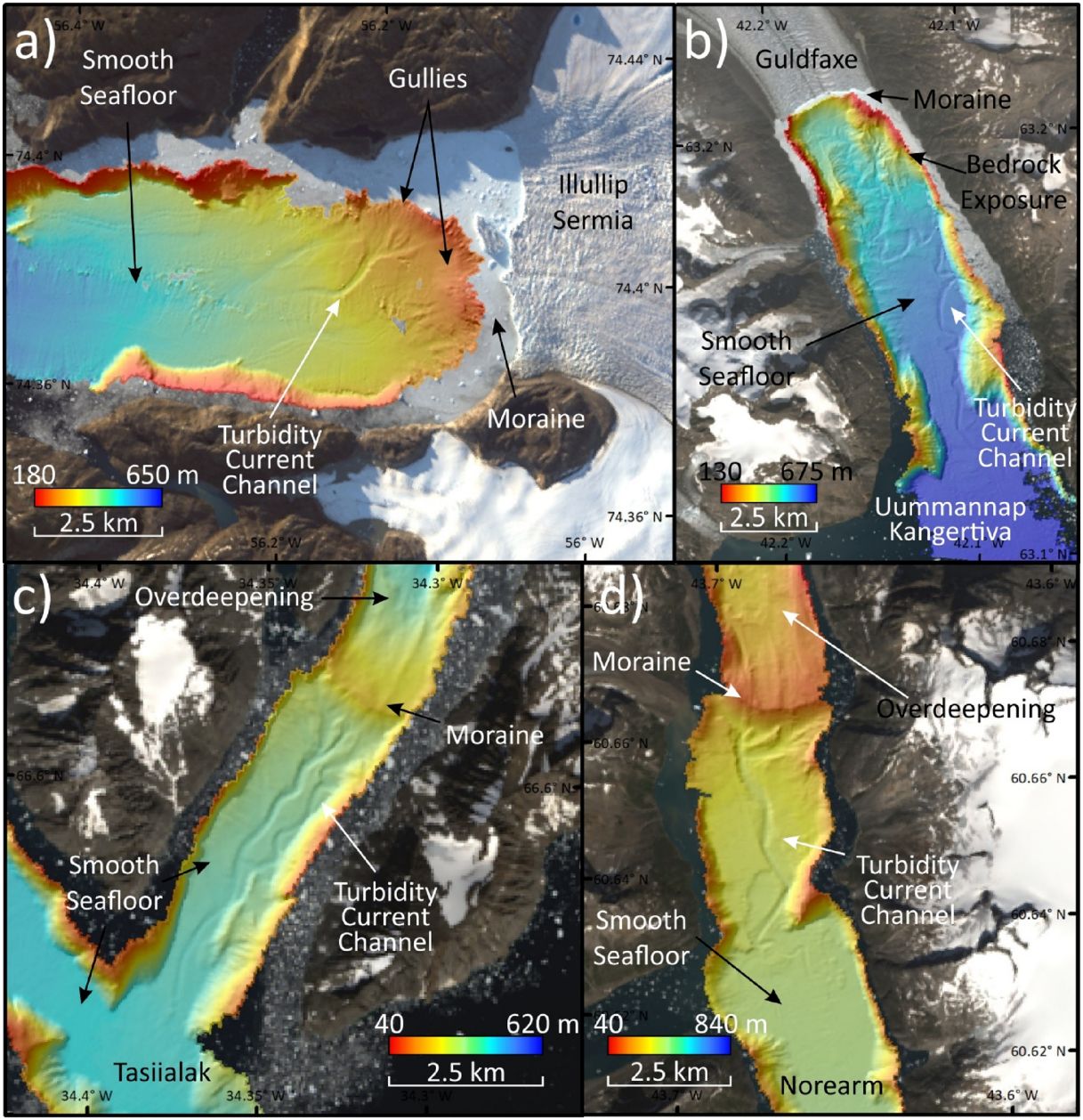
a)
Smooth Seafloor
Gullies
Illullip Sermia
Moraine
Turbidity Current Channel
180
650 m
2.5 km
b)
Guldfaxe
Moraine
Bedrock Exposure
Smooth Seafloor
Turbidity Current Channel
130
675 m
2.5 km
Uummannap Kangertiva
c)
Overdeepening
Moraine
Smooth Seafloor
Turbidity Current Channel
40
620 m
2.5 km
Tasiialak
d)
Moraine
Overdeepening
Turbidity Current Channel
Smooth Seafloor
40
840 m
2.5 km
Norearm

Figure 6

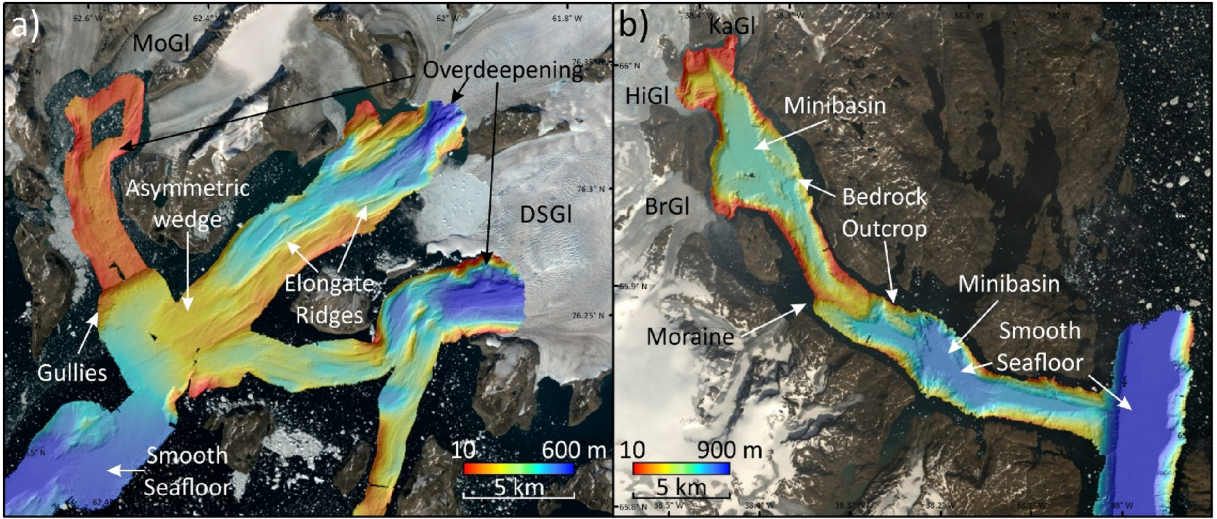
a)
MoGl
Overdeepening
Asymmetric wedge
DSGl
Elongate Ridges
Gullies
Smooth Seafloor
10
600 m
5 km
b)
KaGl
HiGl
Minibasin
BrGl
Bedrock Outcrop
Minibasin
Moraine
Smooth Seafloor
10
900 m
5 km

Figure 7

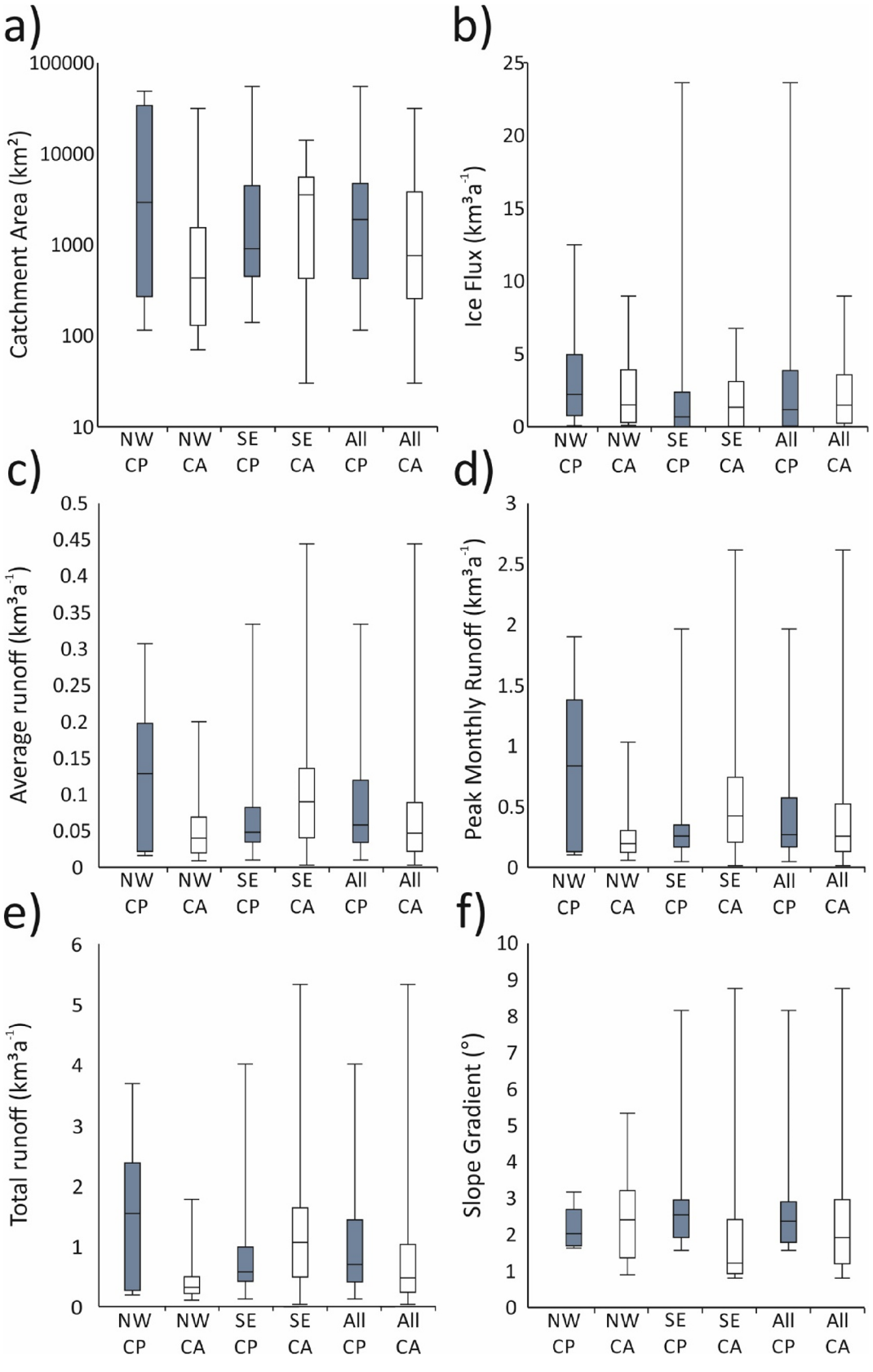
a)
Catchment Area (km²)
100000
10000
1000
100
10
b)
Ice Flux (km³a⁻¹)
25
20
15
10
5
0
c)
Average runoff (km³a⁻¹)
0.5
0.45
0.4
0.35
0.3
0.25
0.2
0.15
0.1
0.05
0
d)
Peak Monthly Runoff (km³a⁻¹)
3
2.5
2
1.5
1
0.5
0
e)
Total runoff (km³a⁻¹)
6
5
4
3
2
1
0
f)
Slope Gradient (°)
10
9
8
7
6
5
4
3
2
1
0
NW CP
NW CA
SE CP
SE CA
All CP
All CA

Figure 8

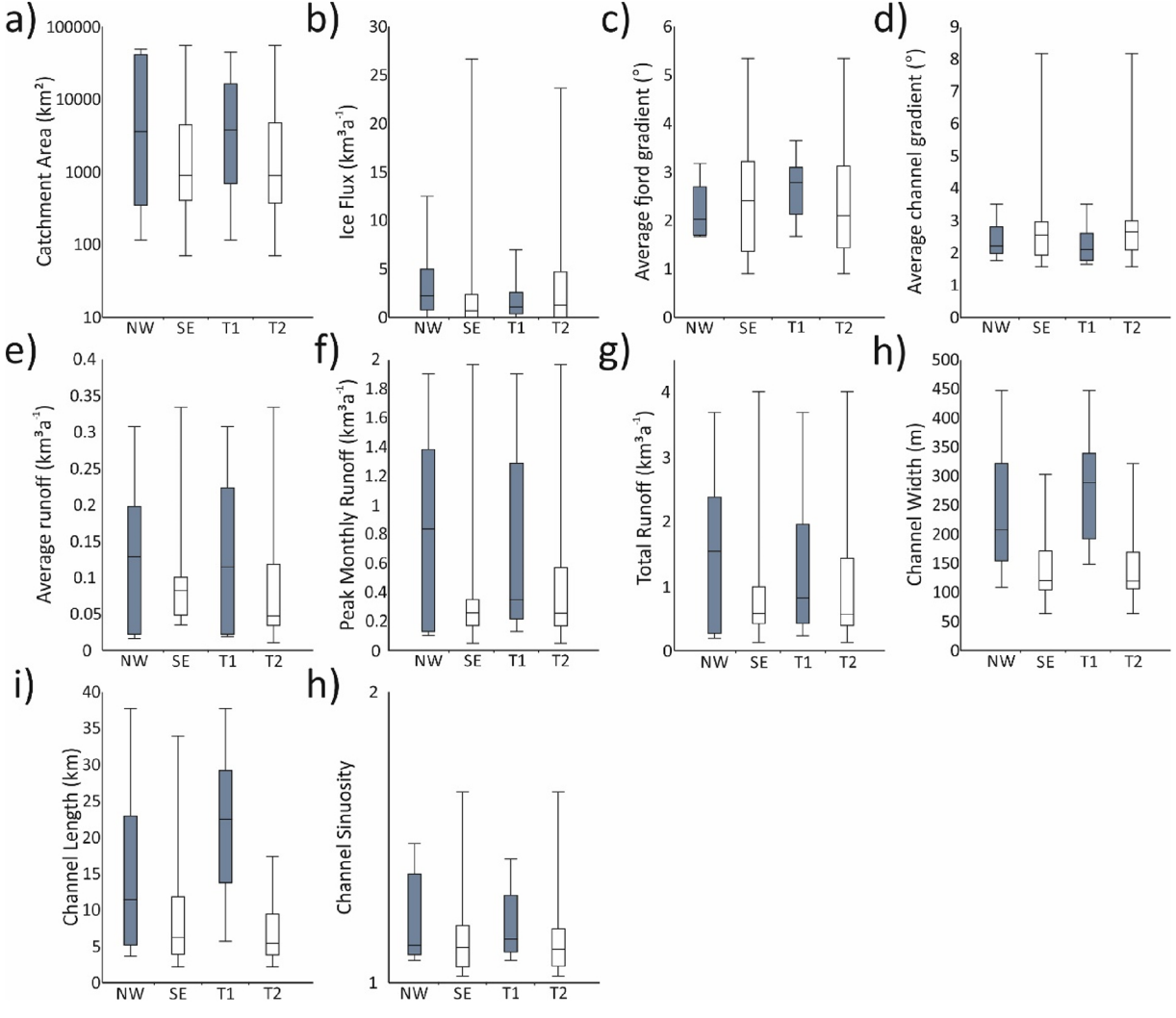
a)
Catchment Area (km²)
100000
10000
1000
100
10
NW
SE
T1
T2
b)
Ice Flux (km³a⁻¹)
30
25
20
15
10
5
0
c)
Average fjord gradient (°)
6
5
4
3
2
1
0
d)
Average channel gradient (°)
9
8
7
6
5
4
3
2
1
0
e)
Average runoff (km³a⁻¹)
0.4
0.35
0.3
0.25
0.2
0.15
0.1
0.05
0
f)
Peak Monthly Runoff (km³a⁻¹)
2
1.8
1.6
1.4
1.2
1
0.8
0.6
0.4
0.2
0
g)
Total Runoff (km³a⁻¹)
4
3
2
1
0
h)
Channel Width (m)
500
450
400
350
300
250
200
150
100
50
0
i)
Channel Length (km)
40
35
30
25
20
15
10
5
0
h)
Channel Sinuosity
2
1

Figure 9

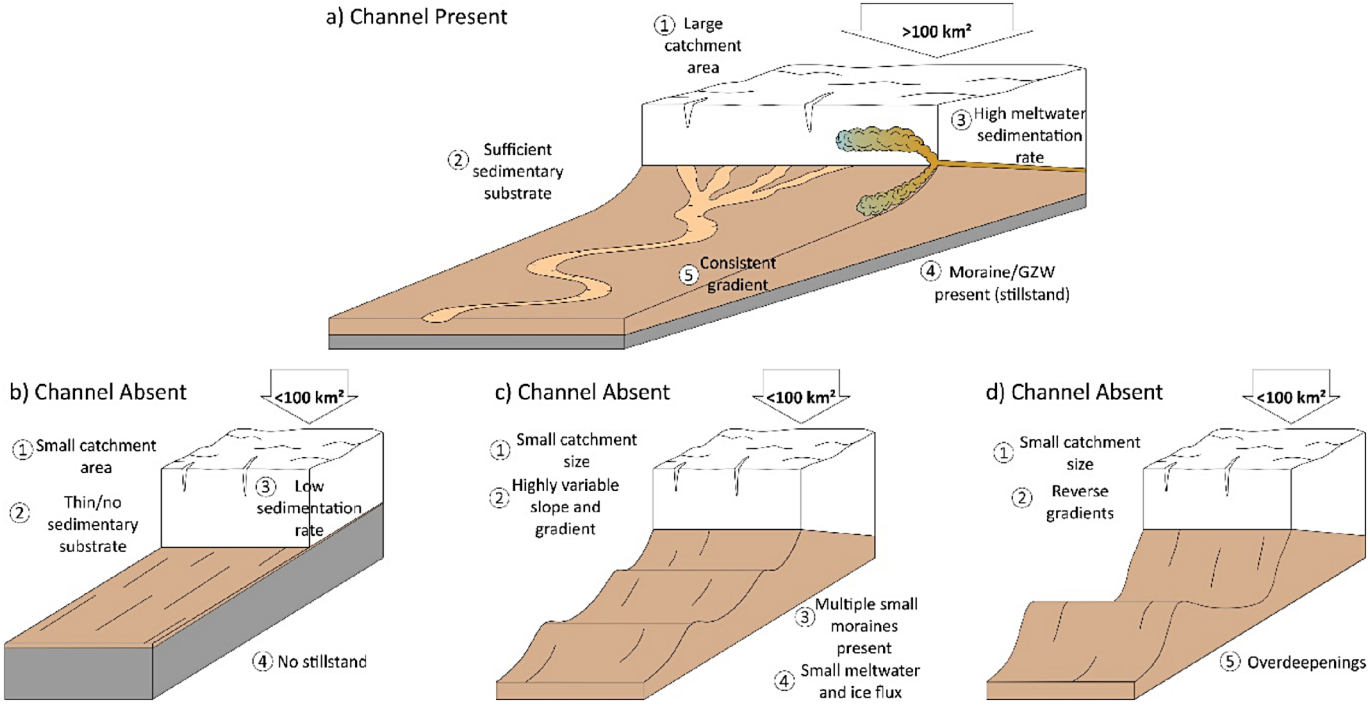
a) Channel Present
1 Large catchment area
>100 km²
2 Sufficient sedimentary substrate
3 High meltwater sedimentation rate
5 Consistent gradient
4 Moraine/GZW present (stillstand)
b) Channel Absent
<100 km²
1 Small catchment area
2 Thin/no sedimentary substrate
3 Low sedimentation rate
4 No stillstand
c) Channel Absent
<100 km²
1 Small catchment size
2 Highly variable slope and gradient
3 Multiple small moraines present
4 Small meltwater and ice flux
d) Channel Absent
<100 km²
1 Small catchment size
2 Reverse gradients
5 Overdeepenings

Figure 10

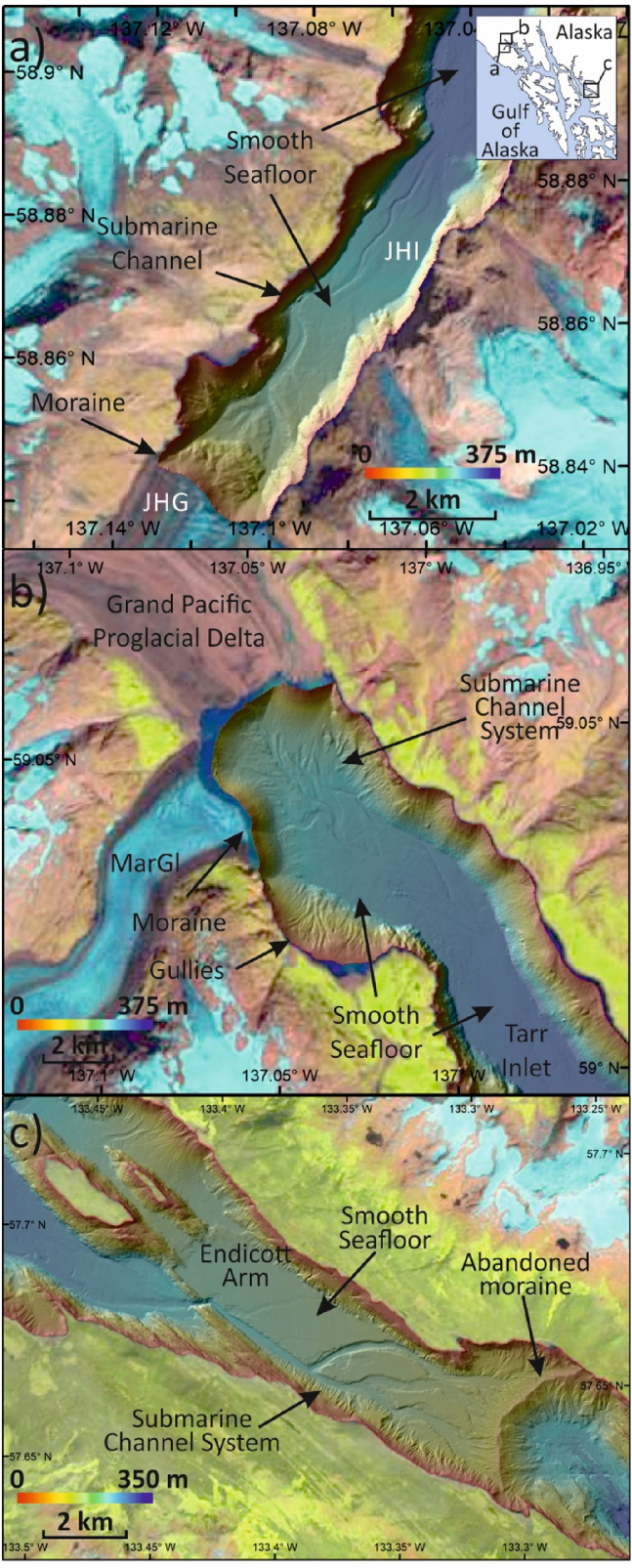
a)
137.12° W
137.08° W
137.0
58.9° N
58.88° N
58.86° N
58.84° N
137.14° W
137.1° W
137.06° W
137.02° W
Smooth Seafloor
Submarine Channel
JHI
JHG
Moraine
0
375 m
2 km
Alaska
Gulf of Alaska
a
b
c
b)
137.1° W
137.05° W
137° W
136.95°
59.05° N
59° N
Grand Pacific Proglacial Delta
Submarine Channel System
MarGl
Moraine
Gullies
Smooth Seafloor
Tarr Inlet
0
375 m
2 km
c)
133.45° W
133.4° W
133.35° W
133.3° W
133.25° W
57.7° N
57.65° N
Endicott Arm
Smooth Seafloor
Abandoned moraine
Submarine Channel System
0
350 m
2 km

Figure 11